

Transformer Design Considerations Utilising Natural Ester Oils

Seeralin Nayager

12/03/2018

In fulfilment of the Masters of Science, College of Agriculture, Engineering and Science, University
of KwaZulu-Natal

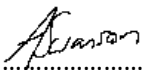
COLLEGE OF AGRICULTURE, ENGINEERING AND SCIENCE

DECLARATION 1 –Supervisor Agreement

I, Andrew Swanson, declare that

1). I hereby verify that I have reviewed the final version of this thesis and approve this submission

Signed


.....

COLLEGE OF AGRICULTURE, ENGINEERING AND SCIENCE

DECLARATION 2 - PLAGIARISM

I, Seeralin Nayager, declare that

1. The research reported in this thesis, except where otherwise indicated, is my original research.
2. This thesis has not been submitted for any degree or examination at any other university.
3. This thesis does not contain other persons' data, pictures, graphs or other information, unless specifically acknowledged as being sourced from other persons.
4. This thesis does not contain other persons' writing, unless specifically acknowledged as being sourced from other researchers. Where other written sources have been quoted, then:
 - a. Their words have been re-written but the general information attributed to them has been referenced
 - b. Where their exact words have been used, then their writing has been placed in italics and inside quotation marks, and referenced.
5. This thesis does not contain text, graphics or tables copied and pasted from the Internet, unless specifically acknowledged, and the source being detailed in the thesis and in the References sections.

Signed



.....

COLLEGE OF AGRICULTURE, ENGINEERING AND SCIENCE

DECLARATION 3 - PUBLICATIONS

DETAILS OF CONTRIBUTION TO PUBLICATIONS that form part and/or include research presented in this thesis (include publications in preparation, submitted, in press and published and give details of the contributions of each author to the experimental work and writing of each publication)

Publication 1

A Singh, B Mgqubeni, R Govender, G Molabe, A.G Swanson, S Nayager, "Natural Ester Oil Power Transformer Solution for PPC Slurry Substation in Eskom's North West Operation Unit," Cigre Southern African Conference, 2017

Publication 2

S. Nayager, A. Singh, A.G. Swanson, "Multiphysics Simulation of Mineral and Ester Based Transformer Winding," SAUPEC Conference, Johannesburg, South Africa, 2018

Publication 3

S. Nayager, A. Singh, A.G. Swanson "FEM Dielectric Simulation of Mineral and Ester Based Transformer Winding," SAUPEC conference, Johannesburg, South Africa, 2018

Signed:



Abstract

As modern day transformer designs are gradually moving towards an eco-friendly alternate insulation medium, this dissertation is focussed on the modelling of a typical 88/6.6 kV 20 MVA high voltage winding in both FEMM and COMSOL software packages to where the thermal and dielectric the performance of mineral and ester oil were assessed.

For the dielectric analysis, Finite Element Model (FEM) software was utilised and electric field stress measurements (long and short gap) were taken between the windings, paper and pressboard for both ester and mineral oil. Results showed that for natural ester oil, the electrical stresses were concentrated in the paper as opposed to mineral oil where the stresses are more concentrated in the oil. Also a comparison between thermally upgraded (higher permittivity) and standard kraft paper yielded a 1 kV/mm reduction in electric stress for the upgraded kraft paper. This means that transformers with natural ester oil will require more insulation on the windings and greater distances between live and ground paths. For the thermal analysis, the material used was mineral oil and ester oil, with the latter having a higher viscosity. The results indicate that the cooling of the transformer is highly dependent on the velocity of the fluid (thermal transfer through convection). The study showed that for the same inlet velocity of fluid the velocities differed slightly due to the viscosity, but they ultimately had a similar thermal performance. The entire transformer, including radiators, would need to be considered to determine the correct flow and thermal performance for the ester.

Table of Contents

1. Introduction	1
1.1. Research Question.....	2
1.2. Hypothesis	2
1.3. Importance of Study and Contribution	2
1.4. Dissertation Structure	3
2. Literature Review.....	4
2.1. Transformer Introduction.....	4
2.1.1 Core.....	4
2.1.2 Windings	5
2.1.2.1. Oil flow within the windings	6
2.1.3. Insulation Medium.....	7
2.1.4. Cooling	9
2.1.5. Thermal Performance of a Power Transformer.....	10
2.2. Natural Ester Fluid	14
2.2.1 Natural Ester Fluid: Envirotemp FR3 Fluid by Cargill	14
2.2.2 Natural Ester Fluid: MIDELEn.....	15
2.2.3 Natural Ester Fluid: ABB Biotemp	16
2.3. Thermal Design Considerations	17
2.3.1 Viscosity	17
2.3.2 Thermal Ageing and Degradation	17
2.3.2.1 Thermal Design Case Study 1.....	17
2.3.2.2 Thermal Design Case Study 2.....	20
2.3.2.3 Thermal Design Case Study 3.....	21
2.4. Dielectric Design Considerations	22
2.4.1. General Considerations for Transformer Insulation Design	22
2.5. Considerations for Ester Design.....	26
2.5.1 Relative Permittivity.....	26

2.5.2 Breakdown Voltage.....	26
2.5.3 Streamer and Long Gap Breakdown of Natural Ester Fluid	27
2.5.4. Cumulative Creep.....	28
2.5.5. Dielectric Design Case Studies	29
2.5.5.1 Dielectric Design Case Study 1	29
2.5.5.2 Dielectric Design Case Study 2	29
2.5.5.3 Dielectric Design Case Study 3	31
2.6 Summary	32
3 Transformer and Winding Design	33
3.1 Winding Arrangement.....	33
3.2 HV and LV Winding Phase Currents	33
3.3 Core Dimensions and Volts per Turn	34
3.4 Winding Design	35
3.4.1 Dielectric Clearances.....	35
3.4.2 LV Winding Dimensions	36
3.4.3 HV Winding Dimensions.....	38
4. Simulation and Results.....	39
4.1. Dielectric Simulation using FEM Model	39
4.1.1. Results.....	44
4.1.1.1 Simulation 1	44
4.1.1.2 Simulation 2	45
4.2. Thermal Simulation of Mineral and Ester Based Transformer Winding.....	49
4.2.1 Heat Model	52
4.2.2. Heat Model Results.....	54
4.3. Summary of Design Considerations	58
5. Conclusion.....	59
6. References	61
Appendix A.....	65

A.1. FEMM Dielectric Simulations.....	65
A.2. Dielectric simulation code using Octave 4.2.1 software	76
A.3. 88/6.6kV 20MVA Transformer calculation code using Octave 4.2.1 software	77

List of Figures

Figure 1- Typical oil flow for disc and helical windings [12]	7
Figure 2-Transformer Cooling Class Letter Code [8].....	10
Figure 3-Thermal diagram for temperature rise calculations [18]	11
Figure 4-LV/HV Winding Insulation Design Considerations [27]	24
Figure 5- Winding configuration	33
Figure 6 - Winding layout showing	35
Figure 7-LV conductor strand layout	37
Figure 8-Flowchart of insulation system design for dielectric simulations	40
Figure 9-Flowchart of insulation system design for dielectric simulations	41
Figure 10-Transformer geometry with mesh applied.....	42
Figure 11-Boundary- Earth set to zero voltage.....	42
Figure 12-Ester oil assigned a permittivity.....	43
Figure 13-Assigned permittivity per material	43
Figure 14- (left) Mineral Oil-HV to LV winding path-Top section; (right) Ester Oil-HV to LV winding path-Top section	44
Figure 15-Electric field vs Path Length for mineral and ester oils (HV to LV winding path)	45
Figure 16-(left) Mineral Oil-HV to LV winding path-Middle section; (right) Ester Oil-HV to LV winding path-Middle section.....	46
Figure 17-Electric field vs Path Length for mineral and ester oils (HV to LV winding path)	46
Figure 18-(left) Mineral Oil dielectric stresses with thermally upgraded kraft paper; (right) Ester Oil dielectric stresses with thermally upgraded kraft paper	47
Figure 19-Electric field vs Path Length for mineral and ester oils with improved kraft paper	48
Figure 20-Flowchart showing components required for thermal model	52
Figure 21- Geometry of Model	53
Figure 22-(left) Winding heat distribution for mineral oil; (right) Winding velocity distribution for mineral oil	54
Figure 23-Temperature along central and side paths for inlet velocity of 1 mm/s.....	55
Figure 24-Velocity along central and side paths for inlet velocity of 1 mm/s	55
Figure 25- Mineral Oil (HV to LV winding path_Top section)	65
Figure 26-Ester Oil (HV to LV winding path_Top section).....	65
Figure 27-Electric field vs Path Length (HV to LV winding path_Top section).....	65
Figure 28-Mineral Oil (HV to LV winding path_Top section)	66
Figure 29-Ester Oil (HV to LV winding path_Top section).....	66

Figure 30-Electric field vs Path Length (HV to LV winding path_Top section).....	66
Figure 31-Mineral Oil (HV winding to Core path)	67
Figure 32-Ester Oil (HV winding to Core path).....	67
Figure 33-Electric field vs Path Length (HV winding to Core path).....	67
Figure 34-Mineral Oil (HV to LV winding path_Top section_2nd winding disc)	68
Figure 35-Ester Oil (HV to LV winding path_Top section_2nd winding disc)	68
Figure 36-Electric field vs Path Length (HV to LV winding path_Top section_2nd winding disc).....	68
Figure 37-Mineral Oil (HV to LV winding path_Top section_3rd winding disc).....	69
Figure 38-Ester Oil (HV to LV winding path_Top section_3rd winding disc)	69
Figure 39-Electric field vs Path Length (HV to LV winding path_Top section_3rd winding disc)	69
Figure 40-Mineral Oil (HV to LV winding path_Middle section).....	70
Figure 41-Ester Oil (HV to LV winding path_Middle section)	70
Figure 42-Electric field vs Path Length (HV to LV winding path_Middle section).....	70
Figure 43-Mineral Oil (HV to LV winding path_Middle section).....	71
Figure 44-Ester Oil (HV to LV winding path_Middle section)	71
Figure 45-Electric field vs Path Length (HV to LV winding path_Middle section).....	71
Figure 46-Mineral Oil (HV to LV winding path_Bottom section)	72
Figure 47-Ester Oil (HV to LV winding path_Bottom section)	72
Figure 48-Electric field vs Path Length (HV to LV winding path_Bottom section).....	72
Figure 49-Mineral Oil (HV to LV winding path_Bottom section)	73
Figure 50-Ester Oil (HV to LV winding path_Bottom section)	73
Figure 51-Electric field vs Path Length (HV to LV winding path_Bottom section).....	73
Figure 52-Mineral Oil (HV to LV winding path_Bottom section	74
Figure 53-Ester Oil (HV to LV winding path_Bottom section)	74
Figure 54-Electric field vs Path Length (HV to LV winding path_Bottom section).....	74
Figure 55-Mineral Oil (HV to HV winding_1st winding disc to 2nd winding disc)	75
Figure 56-Ester Oil (HV to HV winding_1st winding disc to 2nd winding disc).....	75
Figure 57-Electric field vs Path Length HV to HV winding_1st winding disc to 2nd winding disc)	75

List of Tables

Table 1-Typical characteristics of mineral oil as per IEC 60076-1 [13]	8
Table 2-Temperature Rise Test Calculations as per IEC 60076-7 [18]	13
Table 3-Envirotemp FR3 fluid and specification limits for natural ester and mineral oil [21].....	15
Table 4-Conventional Mineral Oil compared to MIDELEn Oil [22].....	16
Table 5-Conventional Mineral Oil compared to BIOTEMP [23].....	16
Table 6-Mineral oil test results for ONAN and ONAF cooling systems [7]	18
Table 7-Natural ester oil test results for ONAN and ONAF cooling systems [7].....	19
Table 8-Comparison of heat run tests for mineral and ester oils using identical transformers [25] ...	20
Table 9- Temperature simulation results of mineral and ester oils for a 10 MVA transformer [26] ...	21
Table 10- LV/HV Insulation Considerations per Section [27].....	25
Table 11-Summary of Thermal and Dielectric Design Considerations for Natural Ester Oil	32
Table 12-Winding and Core Properties.....	34
Table 13- Electrical Properties for Winding and Core.....	36
Table 14- LV Conductor, Core Clearance and Winding Disc Properties.....	37
Table 15-HV Conductor, Core Clearance and Winding Disc Properties.....	38
Table 16-Relative permittivities considered for the insulation design.....	43
Table 17-Thermal Conductivity of Mineral and Ester Oils	50
Table 18-Kinematic Viscosity of Mineral and Ester Oils.....	50
Table 19-Results for inlet velocity of 1 mm/s	56
Table 20-Results for inlet velocity of 5 mm/s	56
Table 21-Results for inlet velocity of 10 mm/s	56

Acronyms

CTC	Continuously Transposed Conductors
IEC	International Electrotechnical Commission
BIL	Basic Insulation Level
DIL	Design Insulation Level
SIL	Switching Insulation Level
CH	Window Height
WH	Winding Height
OLTC	On-Load Tap Changer
PD	Partial Discharge
C_u	Copper
ASTM	American Society for Testing and Materials
BDV	Break Down Voltage
SI	Switching Impulse
LI	Lightning Impulse
AC	Alternating Current
FEM	Finite Element Model
IEEE	Institute of Electrical and Electronic Engineers
LV	Low Voltage
HV	High Voltage
SOV	Stressed Oil Volume

1. Introduction

Power transformers have traditionally used mineral oil for cooling and insulation purposes due to its low cost and availability. With petroleum reserves depleting and increasing environmental sanctions for oil spillages, natural ester oil has emerged as a favourable replacement for mineral based transformer oil. Natural ester oils are bio-degradable and have therefore become a more attractive alternative as the world is striving towards transformers that are more environmental friendly.

Some key advantages of these oils include higher fire/flash points, superior thermal conductivity, is 100% biodegradable and less flammable [1]. IEC publications indicate that natural ester oil transformers have a greater life expectancy which increases the utility's return on investment on the asset [2]. However, there are major downsides as natural esters are more expensive, possess higher viscosities than mineral oil and age rapidly with oxidation [3]. A higher viscosity affects the oil flow through the ducts and channels designed for cooling the transformer. Insulation fluids with high viscosities tend to increase time for solid insulation impregnation and can even prevent full impregnation. Temperature also has a direct influence on the viscosity of oil. When temperature reduces, viscosity increases and vice versa [4]. The effects of poor cooling within a power transformer would result in the insulation materials deteriorating at a rapid rate which could lead to failure.

When designing the insulation of a transformer it is critical that all factors are considered to ensure total system reliability and optimisation of material. Insulation space impacts the cost of the active parts and influences the quantity of the oil within the unit. There have been many comparative literature studies published highlighting the properties between mineral and ester oils whilst a few have analysed the thermal and dielectric effects within a transformer winding [1] [3] [5] [6] [7]. Advanced simulation computational programs such as FEMM and COMSOL are used to accurately calculate electric stress levels and thermal performance of a winding and are then compared to establish withstand specifications. Although the initial cost of ester oil is expensive, implementation would benefit utilities when one considers the total lifecycle cost as one should to remain compliant with the South African Grid Code. With natural ester based transformers, structures such as bund walls/firewalls could be reduced due to the esters biodegradable property.

1.1. Research Question

- What is the thermal behaviour of natural ester oil in comparison to mineral oil for an 88/6.6 kV 20 MVA transformer?
- What is the dielectric behaviour of natural ester oil in comparison to mineral oil for an 88/6.6 kV 20 MVA transformer?
- What general considerations (thermal and insulation) must be taken for adapting a mineral oil transformer to accommodate natural ester oil?

1.2. Hypothesis

The hypothesis is that modifications are required in the mineral oil power transformer to accommodate natural ester oil due to the different thermal and dielectric behaviour.

1.3. Importance of Study and Contribution

The importance of implementing a fully functional natural ester power transformer will benefit power utilities across the world for the following reasons:

- Increased fire safety at substations-minimal damage to surrounding equipment
- The higher flash point of natural esters can reduce build and labour costs at the substation as the IEC specifications allow for reduced clearances
- Oil dams, spillage clean up kits and the associated pipework are no longer needed thus reducing costs
- No harmful impact to environment

1.4. Dissertation Structure

Chapter 2 covers a literature review of the internal components in a power transformer which comprises of the windings, insulation and dielectric systems. Multiple case studies and research from other engineering authors regarding natural ester oil implementation in mineral oil power transformers are discussed.

Chapter 3 covers design calculations of an 88/6.6 kV 20 MVA ONAN power transformer validated from an international manufacturer.

Chapter 4 shows the construction of both thermal and dielectric models in FEMM and COMSOL for an 88/6.6 kV transformer winding. An in depth analysis was conducted from the natural ester/mineral oil research results.

Chapter 5 concludes the dissertation and provides recommendations for a natural ester oil power transformer.

2. Literature Review

2.1. Transformer Introduction

In many distribution and transmission grids around the world, transformers represent a key component and form the largest capital portion within substations. A transformer is a device consisting of one or more windings that converts electrical energy from one circuit to another by means of electromagnetic induction. Its main purpose is to either reduce or step up a voltage to an appropriate level in order to supply respective devices/customers. It comprises of a magnetic core, windings, insulation system and cooling system which form the main four subsystems within a transformer [8].

2.1.1 Core

The main purpose of the core is to link the primary and secondary windings via mutual magnetic flux. This linkage must be one of a low reluctance path which is significant for coupling efficiency and reduced losses. The core experiences two types of losses namely Hysteresis and Eddy Current losses (also known as no load losses). These losses can be represented by heat dissipated within the transformer. Both Hysteresis and Eddy Current losses are proportional to flux density and frequency. The total loss can be represented by the following equation [9]:

$$Loss = Hys_{loss} + Eddy_{loss} = (k_1 \times f \times B^n) + (k_2 \times f^2 \times B^2) \quad (1)$$

Where k_1 and k_2 are constants of proportionality

f is the frequency in Hz

B is flux density in Wb/m^2

n is the value dependent on the characteristic of the magnetic steel

In order to minimize these losses, the core is designed with special grain orientated steel comprising of iron, silicon and other elements. The steel is cut into thin sheets called laminations which are electrically insulated from each other. This increases the resistivity and assists in reducing the eddy current paths [10].

2.1.2 Windings

The windings of a transformer consist of current carrying conductors that are wound around the limbs of the core. These conductors can be arranged in three configurations namely: rectangular, group insulated or continuously transposed. Continuously Transposed Conductors (CTC) is considered mechanically superior than the other arrangements as it offers greater resistance to the distorting effects of short circuit forces [10]. Kraft paper which is manufactured from wood pulp is wrapped around the conductor. When mineral oil is inserted within the transformer it impregnates the paper which provides a basic insulating medium for the winding conductors. Copper and aluminium are the most commonly used material for the winding conductor. Aluminium generally is not used in large transformers due to its brittle properties, lower current carrying capabilities and high resistivity ($2.82 \times 10^{-8} \Omega.m$). Copper on the other hand has higher mechanical strength, current carrying capabilities and contains lower resistivity ($1.72 \times 10^{-8} \Omega.m$) when compared to aluminum [8].

Under load, the flow of current in the windings produce load losses and is determined by the resistance and cross sectional area of the conductor. These losses are given by the following equation [11]:

$$\text{Losses} = I^2 \times R \quad (2)$$

There are three main categories of winding designs which can be implemented in core form transformers. Helical, interleaved and disc winding arrangements are commonly used in power transformers.

Disc winding: Consists of a single conductor or up to several conductors that are wound in a series of parallel discs arranged in a horizontal orientation. This arrangement increases the series capacitance required for overvoltage conditions (lightning or switching surges). The discs are either interconnected on the inside or crossed over points on the outside [8].

Helical winding: Multiple conductors are wound in a simple helix arrangement from one end of the coil to the other. This arrangement assists in reducing stray losses when the transformer experiences overcurrent conditions (short circuit faults) [8].

Interleaved winding: Is made up of ten or more flat conductors with normal insulation paper or transposed conductors. This arrangement is repeatedly wound in the radial direction of the coil, creating a high series capacitance. This is advantageous as it improves efficiency of winding manufacturing as well as decreases eddy current losses. It has been proven that this winding arrangement also displays excellent lightning impulse withstand characteristics which in turn contributes to the reduction of equipment size [10].

2.1.2.1. Oil flow within the windings

The cooling medium (mineral oil) serves the purpose of continuously circulating within the transformer, removing heat from the windings and displacing it into the environment via radiators. Figure 1 shows the flow of mineral oil through the various ducts for an HV/LV winding. The arrows in represent the typical oil flow patterns in the windings and tank of a transformer. It can be seen that oil flows vertically up through the following cooling ducts: radial HV and LV, HV to LV as well as the LV to core. Within the winding there are also horizontal oil flows between the coil segments. This horizontal arrangement is commonly found in disc and helical winding configurations. Additionally, manufacturers use flow washers within the windings to orientate horizontal oil further [12].

The transfer flow of heat from the windings to the oil affects the density of the oil. When oil enters the winding from the bottom moving up, heat is absorbed resulting in the decrease of the oil density. Further heat is absorbed as the oil continues to move further up the winding reaching the top. The oil over the top of the windings then channels itself through the cooling systems via the transformer tank and radiators where it is cooled down.

By the time the oil reaches the bottom of the tank it becomes denser in volume and the process repeats itself [12]. Most transformer designers use disc and helical windings as it provides the winding conductors with maximum exposure to the circulating oil. In Figure 1, the radial spacers and end rings which are generally used for winding support also supply every conductor with oil flow. Spacer thickness must be designed to provide efficient cooling and decrease winding temperature rise. Furthermore, depending on which type of cooling system is used, directed oil flow through the windings will improve the cooling performance of the transformer [12].

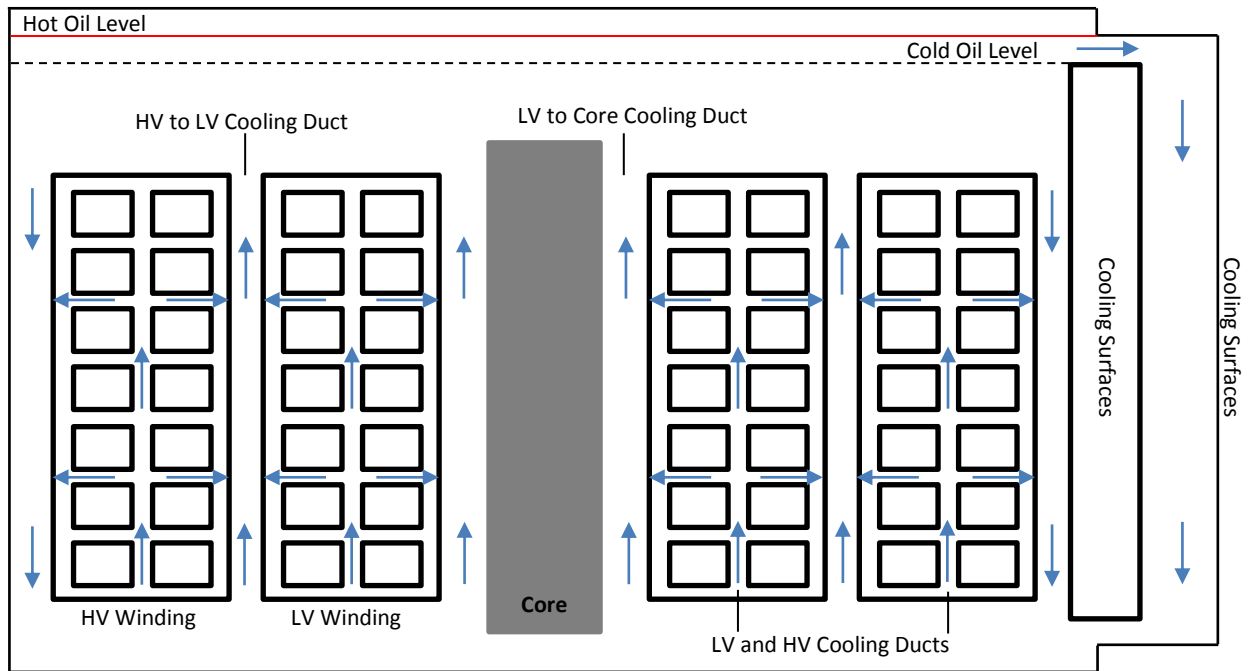


Figure 1- Typical oil flow for disc and helical windings [12]

2.1.3. Insulation Medium

For many decades, power transformers have used mineral oil due to its low cost and availability. Mineral oil is a petroleum based product manufactured from refining crude oil. Refining is the process of changing crude oil, with specified properties, into insulating oil [8]. Mineral oil forms the bulk content of the main tank surrounding the core, windings and insulating material and serves the following functions:

- Provides insulation between high potential barriers in the transformer system
- Provides a cooling medium in the transformer system
- Provides internal information on the health of the transformer

The chemical properties of mineral oil can comprise of naphthenic (C_nH_{2n}), paraffinic (C_nH_{2n+2}) or aromatic (C_nH_{2n-6}) structures. Some common mineral oil manufacturers include Engen, Shell and Nynas which provide various products ranging from inhibited to non-inhibited oils.

Table 1-Typical characteristics of mineral oil as per IEC 60076-1 [13]

Generic Name	IEC Standard	Thermal Class °C	Flash Point °C	Fire Point °C	Water Content mg/kg	Relative Permittivity at 25°C	Kinematic Viscosity mm ² /sec		Thermal Conductivity at 25°C W/mK	Specific Heat at 25°C J/kg °C
							At 40°C	At 100°C		
Mineral oil	60296	105	145	160	25	2.2	9.2	2.3	0.12	2100

Table 1 is an extract from standard IEC 60076-1 which indicates the typical accepted properties of mineral oil with associated definitions.

Flash point: Is the lowest temperature at which an ignition source causes the vapours of the specimen (lubricant) to ignite under specified conditions [14].

Fire point: The fire point is the lowest temperature beyond the flash point at which the mixture of vapours and oxygen will burn continuously if ignited [15].

Viscosity: Viscosity influences heat transfer and therefore temperature rise of the equipment. The lower the viscosity, the easier the oil circulates leading to improved heat transfer [16].

Pour point: Is the lowest temperature at which oil will flow [16].

Water content: Is the maximum quantity of water that is acceptable in mineral oil [11].

Thermal Conductivity: Is the ability of mineral oil to conduct heat [8]

From Table 1 the important properties to note is that mineral oil contains a flash point of 145 °C, fire point of 160 °C, water content of 25 mg/kg and kinematic viscosities which vary between 9.2 mm²/sec and 2.3 mm²/sec depending on the temperature. The dielectric strength in oil refers to the maximum electric strength it can withstand continuously without losing its insulating properties. This insulation is controlled mainly by the complex paper/oil structures within the transformer.

The oil has the important function of impregnating all cellulose components such as insulation paper, pressboard and wood hence displacing the air which contains a lower dielectric strength than mineral oil. The breakdown voltage also serves as an indicator for determining the efficiency of the oil which can be influenced by impurities such as moisture, foreign particles and combustible gases.

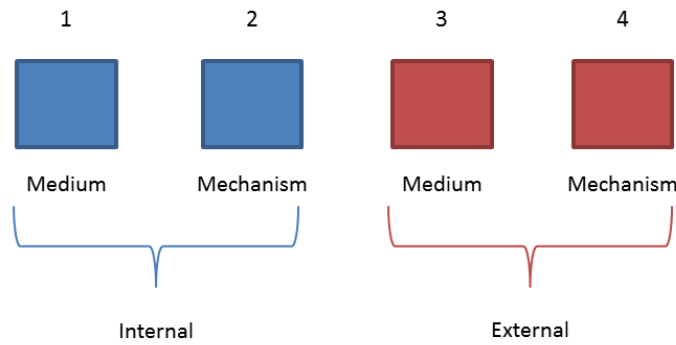
The dielectric test is governed by the IEC 60156 standard which involves determining the voltage at the point when sparks are produced between two oil immersed electrodes 2.5 mm apart [5] [17].

Kinematic viscosity in the context of oil can be defined as the resistance to flow and is the most influential parameter for heat transfer within a transformer. Oil with lower kinematic viscosities will generally improve cooling performance when compared to oil with higher viscosities due to reduced thickness (better flow rate) in chemical composition. Insulating fluids with high viscosities tend to increase time for solid impregnation and could prevent full impregnation. Temperature has a direct influence on the viscosity of oil. When temperature reduces, viscosity increases and when temperature increases, viscosity decreases in oil [4].

2.1.4. Cooling

The windings and core are the main producers of heat within a transformer which results in energy loss. If this heat is sustained for long durations it will lead to the deterioration of the paper insulation in the windings. Therefore, it is imperative that the transformer windings contain essential ducts and passages for oil to flow so that heat can be removed. Most transformers rely on the thermosiphon effect which is the natural circulation of oil in the transformer through convection. Oil is circulated within the transformer and heat is dissipated to the environment via the tank walls and radiators which assists in increasing the surface dissipation area.

Transformers consist of a variety of enhanced cooling and oil distribution configurations depending on the application and size. Fans can be attached to the transformer to increase the volume of air through the radiators thus improving heat dissipation from the oil. With larger transformers, pumps are used to direct the flow of oil through the windings. The IEC 60076-1 has stipulated a four letter standard designation for cooling classes [13]. Figure 2 shows the different types of cooling classes a power transformer can possess. Some common examples of the above classifications include: ONAN (Oil Natural Air Natural), ONAF (Oil Natural Air Forced), ODAF (Oil Directed Air Forced) and OFAF (Oil Forced Air Forced) transformers.



1st Letter: Type of Cooling Medium (Internal)

O = Oil

2nd Letter: Method of Cooling (Internal)

N = Natural Circulation

D = Directed by pumps

3rd Letter: Type of Cooling Medium (External)

A = Air

W = Water

4th Letter: Circulation Type of External Medium

N = Natural Circulation

Figure 2-Transformer Cooling Class Letter Code [8]

2.1.5. Thermal Performance of a Power Transformer

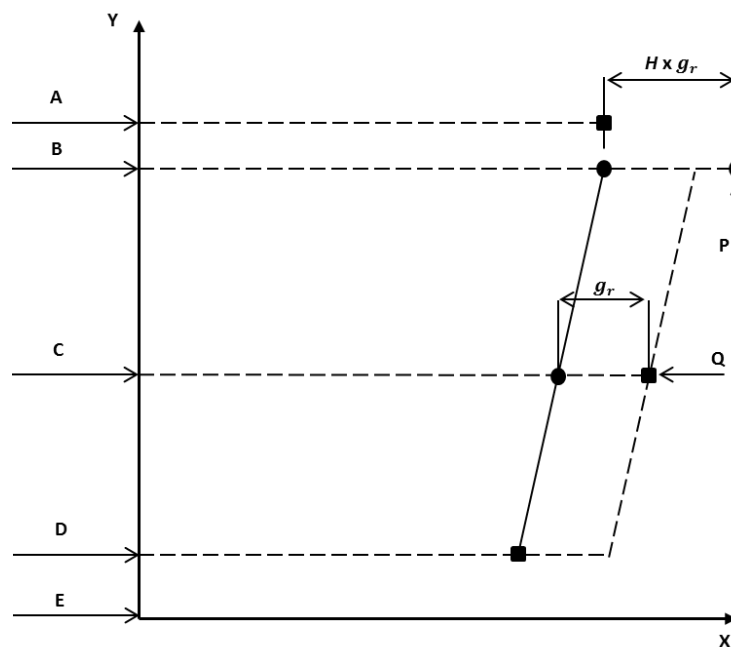
The core and winding losses generated in the form of heat contributes to the deterioration of the insulation system within a power transformer. It is therefore essential that the cooling system maintains the thermal performance ensuring that the winding insulation is never compromised. The thermal performance of a power transformer is generally measured by calculating the hot spot temperature in the winding and determining the cooling medium temperature. The hot spot temperature rise test is used to calculate the average temperature rise of the windings above ambient temperature when loaded to its nameplate rating.

It is calculated by methods stipulated in the IEC 60076-7 standard or by direct measurements using optical fibre sensors. This test evaluates the winding lifespan of a transformer and is directly affected by loading in conjunction with the duration, as well as cooling parameters [5] [18].

During a temperature rise test the following values are measured to evaluate the aging of a winding [5]:

- Top oil temperature (θ_o)
- Mean winding temperature (θ_w) which is measured by the winding resistance variation during the temperature rise test
- Ambient temperature (θ_A)

The top oil winding temperature for most transformers in service is not precisely known when compared to the top oil temperature of the tank which can be calculated or measured. Past trends from measurements have indicated that the top oil temperature inside a winding (cooling dependent) is about 15 K hotter than the top oil temperature of the tank [3]. The IEC 60076-7 standard provides a simplified diagram (see Figure 3) of a complex transformer thermal system.



Legend for Temperature Rise Test Thermal Diagram	
Key	Description
A	Top Oil Temperature
B	Top of Winding-Mixed Oil Temperature
C	Average Oil Temperature in Tank
D	Bottom of Winding-Oil Temperature
E	Bottom of Tank
gr	Average Winding to Average Tank Oil Temperature gradient at rated current
H	Hot Spot Factor
P	Hot Spot Temperature
Q	Average Winding Temperature determined by resistance measurement

Figure 3-Thermal diagram for temperature rise calculations [18]

Assumptions are made for simplification and take into account the following [18]:

- There is a linear increase from bottom to top of the oil temperature within the tank, irrespective of the cooling mode.
- At any position up the winding, the temperature rise of the conductor will increase linearly. This will be parallel to the oil temperature rise with a constant difference of g_r between the two straight lines.
- Due to allowances for stray losses, differences in oil flow and additional paper on the conductor, the hot spot temperature rise at the top of the winding will be higher than the temperature rise of the conductor.
- To compensate for non-linearities, the difference in hot spot and top oil temperatures is equated to the hot spot factor H multiplied by g_r .

Figure 3 is extracted from the IEC 60076-7 standard and shows a plot of temperature (x axis) against relative positions (y axis) on a winding. The square visuals represent a measured point whilst the circle visuals represent a calculated point. The constant g_r is the difference between the winding (by resistance) and oil (in tank) average rise temperatures. The hot spot factor H varies per winding and must be calculated on a case by case basis. Depending on the size of the transformer, H varies within the range of 1.0 and 2.1. The hot spot factor H can be either defined by direct measurement or by calculation using fundamental loss and heat transfer principles.

If using the calculation method the following factors must be considered [17] [19] :

- For each winding cooling duct - The flow rate, heat transfer and resultant fluid temperature must be modelled.
- Losses in the winding due to radial flux eddy losses (interception of leakage flux with wide dimension conductor), eddy and circulating current losses, D.C. resistance losses and leakage flux heating.
- Conduction heat transfer effects within the winding which can be induced by different insulation thickness used throughout the winding or flow directing washers for zigzag winding configurations.

Taking into account the previous considerations, Table 2 below represents a summary of the IEC 60076-7 temperature rise calculation loading guide that designers can use to calculate the relevant parameters [18]

Table 2-Temperature Rise Test Calculations as per IEC 60076-7 [18]

Description	Symbol	Calculation
Top oil temperature rise	$\Delta\theta_{Or}$	$\theta_O - \theta_A$
Mean winding temperature rise	$\Delta\theta_W$	$\theta_W - \theta_A$
Mean oil temperature	$\Delta\theta_{OM}$	$0.8 \times \Delta\theta_{Or}$
Mean winding/Oil gradient	g_r	$\Delta\theta_W - \Delta\theta_{OM}$
Top winding hot spot gradient	$\Delta\theta_{hgr}$	$H \times g_r$
Hot spot winding temperature	θ_{hr}	$\theta_A + \Delta\theta_{hr}$
Hot spot winding temperature rise	$\Delta\theta_{hr}$	$\Delta\theta_{Or} + \Delta\theta_{hgr}$

2.2. Natural Ester Fluid

For many decades, transformers have used mineral oil for cooling and insulation purposes due to its low cost and availability. With petroleum reserves depleting and increasing environmental sanctions, natural esters have emerged as a favourable replacement for mineral based transformer oil. Apart from being eco-friendly, natural ester oils have become a more attractive alternative to electrical utilities due to its superior properties. Natural ester oil is manufactured from plant crops (soya, rape seeds and sunflower oil) and consists of a glycerol backbone to which fatty acid groups are attached. Some key advantages of natural ester oil over mineral oil include [3]:

- Contains higher fire and flash points
- Superior thermal conductivity
- 100% biodegradable
- Less flammable

However, there are downsides as natural esters are more expensive, possess higher viscosities than mineral oil and ages rapidly with oxidation. Although the initial cost of ester oil is expensive, implementation will benefit utilities with environmental sanctions.

2.2.1 Natural Ester Fluid: Envirotemp FR3 Fluid by Cargill

Insulating fluids serve two important functions of which one is providing electrical insulation and the other to ensure the internals of the transformer is cooled effectively. These two functions are strongly dependent on the dielectric breakdown voltage and viscosity properties of the insulating fluid. The dielectric breakdown is a measure of the electrical insulation effectiveness whilst the viscosity influences the cooling performance of the oil. For this study, Envirotemp FR3 fluid will be the natural ester of choice and shall be used to model the heat distribution and dielectric characteristics of an 88/6.6 kV 20 MVA mineral oil transformer. Envirotemp FR3 fluid is a dielectric coolant which is intended for power transformer use as it's not harmful to the environment if spilled, contains superior fire point resistance, and its electrical properties is advantageous [20]. Envirotemp Bulletin B900-00092 indicates that FR3 fluid does not contain any petroleum, halogens or silicone properties when compared to mineral oil. The chemical composition of FR3 fluid is a mixture of polar triglycerides and readily forms of hydrogen bonds [21].

Apart from the superior flash and fire points to mineral oil, the manufacturer also stipulates that FR3 fluid reaches 40% relative saturation at an absolute water content of 400 mg/kg [21]. This means that the FR3 fluid can absorb approximately 16 times more moisture than mineral oil before saturation occurs. As mentioned earlier, one major disadvantage that the FR3 fluid possesses is that it contains a higher kinematic viscosity than mineral oil which could potentially affect the flow rate of oil.

Table 3, provided by the FR3 Fluid manufacturer Cargill, compares newly processed FR3 fluid to that of ASTM specifications for natural ester and mineral oils. From Table 3 it can be seen that the FR3 fluid dielectric breakdown properties meet both 1 mm and 2 mm gap requirements as per ASTM D1816 specifications.

Table 3-Envirotemp FR3 fluid and specification limits for natural ester and mineral oil [21]

Test	ASTM Method	Historical Range for New Processed FR3 Fluid Prior to Packaging	Specification for New Natural Ester ASTM D6871	As-Received Fluid Mineral Oil ASTM D387
Dielectric Breakdown [kV]	D877	42-48	≥ 30	≥ 30
1mm gap	D1816	25-37	≥ 20	≥ 20
2mm gap		50-75	≥ 35	≥ 35
Volume Resistivity [Ω-cm]	D1169	10-30 x 10 ¹²	-	-
Kinematic Viscosity [mm²/sec]	D445			
40 °C		33-35	≤ 50	≤ 12
100 °C		8.0-8.5	≤ 15	≤ 3
Water Content[mg/kg]	D1533	20-50	≤ 200	≤ 35
Pour Point [°C]	D97	-24 to -21	≤ -10	≤ -40
Acid Number [mg KOH/g]	D974	0.02-0.04	≤ 0.06	≤ 0.03
Gassing Tendency[μl/min]	D2300	-78 to -80	≤ 0	-
Interfacial Tension [mN/m]	D971	20-25	-	≥ 40
Flash Point [°C]	D92	310-330	≥ 275	≥ 145
Fire Point [°C]	D92	350-360	≥ 300	-

2.2.2 Natural Ester Fluid: MIDEL eN

MIDEL eN is a natural ester based insulating fluid which is manufactured from edible seed oil. It is designated to be used in power transformers and is suited for installations where fire safety and environmental sanctions are required. Some important characteristics of MIDEL eN include superior

dielectric breakdown voltages, fire and flash points when compared to conventional mineral oil. It is also fully biodegradable and contains a higher moisture tolerance than mineral oil. The main disadvantage of MIDELE n, which is common with most natural ester oils, is the high kinematic viscosity. Table 4 below highlights the important properties of MIDELE n.

Table 4-Conventional Mineral Oil compared to MIDELE n Oil [22]

Test	Test Methods	MIDELE n	Mineral Oil
Dielectric Breakdown [kV]	ASTM D 1816/ IEC 60156	≥ 75	≥ 70
Kinematic Viscosity [mm ² /sec]	ISO 3104 /ASTM D 445		
100 °C		9.3	2.6
Thermal Conductivity at 20 °C [W/m K]		0.177	0.126
Pour Point [°C]	ISO 3016 /ASTM D 97	≤ -31	≤ - 50
Acid Number [mg KOH/g]	IEC 62021 /ASTM D 974	≤ 0.05	≤ 0.03
Flash Point [°C]	ISO 2592 /ASTM D 92	327	150
Fire Point [°C]	ISO 2592 /ASTM D 92	360	170

2.2.3 Natural Ester Fluid: ABB Biotemp

BIOTEMP insulating fluid which is manufactured by ABB is another natural ester based oil intended for power transformer use. BIOTEMP is manufactured from vegetable oil and comprises of additives to enhance oxidation stability. This natural ester oil is non-toxic and biodegrades (97%) within 21 days. It contains superior flash and fire points but one of major disadvantages is that the kinematic viscosity is substantially higher than conventional mineral oil. Table 5 below highlights the important properties of ABB Biotemp oil.

Table 5-Conventional Mineral Oil compared to BIOTEMP [23]

Test	Test Methods	BIOTEMP	Mineral Oil
Dielectric Breakdown [kV]	ASTM D877	≥ 45	≥ 30
Kinematic Viscosity [mm ² /sec]	ASTM D445		
100 °C		10	3
Thermal Conductivity at 20 °C [W/m K]	ASTM D2717	0.17	0.12
Pour Point [°C]	ASTM D 97	-15 to -25	- 40
Acid Number [mg KOH/g]	ASTM D 974	0.075	0.03
Flash Point [°C]	ASTM D 92	330	145
Fire Point [°C]	ASTM D 92	360	160

2.3. Thermal Design Considerations

2.3.1 Viscosity

Darwin et al. performed viscosity measurements under normal operating temperatures in accordance with the ISO 3104 specification. The results confirmed that transfer of heat by convection within a transformer is less efficient for natural esters because the high viscosity produces slower oil flow rates in the winding ducts [5]. Darwin et al. suggests that oils possessing higher viscosities will operate hotter resulting in rapid cellulose degradation due to slow heat dissipation. The Cigre workgroup for new insulating fluids discuss multiple tests for both natural ester and mineral oil. Their results for viscosity were similar to Darwin et al. findings [24].

2.3.2 Thermal Ageing and Degradation

The ageing of the oil is important for determining the lifetime of the transformer. The characteristics of the oil determine the deterioration of the paper over time. Esters have the ability to hold more water than mineral oil, and hence extend the life of the paper. The natural ester has experimentally been shown to extend the life of the paper or allow a transformer to run at a higher temperature [21].

2.3.2.1 Thermal Design Case Study 1

Bae et al. published a Cigre paper in 2016 focusing on the design of a 154 kV 20 MVA ONAN/ONAF transformer using natural ester oil. Bae et al. conducts an electromagnetic and thermo-fluid analysis for both mineral oil and natural ester fluid based transformers. He highlights two options in transformer design to compensate for the poor cooling performance that is evident for natural ester oil. One could lower the transformer losses by optimizing the magnetic system and winding arrangement or increase the cooling ducts which would consequently expand the winding and tank size. In addition, lowering the transformer losses would require further optimization of the insulation distances and cooling systems. Bae et al. references studies done by Cooper Systems and Fritsche for natural ester fluid. He concurs with their findings which compares permittivities of

cellulose components and different fluids indicating that natural esters contain a higher permittivity than mineral oil making it favourable for insulation purposes. He also agrees that the dielectric strength of natural ester fluids behaves similar to mineral oil when exposed to different voltage stresses (AC, SI and LI) in a homogeneous arrangement [6] [7]. He takes into account Fritsche tests conducted for inhomogeneous arrangements which show that the ratio of related breakdown voltage increases significantly for natural ester oil when compared to mineral oil [3]. Bae et al. uses all these findings to conduct their thermos-fluid and electromagnetic analysis.

Bae et al. uses software by Ansys (Fluent) to develop various models to simulate temperature rise tests for both mineral/natural ester oils and compares this to experimental results. They simulated the oil temperature rise, average winding temperature rise and hot spot temperature rise and thereafter compared it to results from transformers fitted with both ONAN/ONAF cooling systems. Most of the mineral oil tests were done according to IEC 60076-2.

To obtain the most accurate reading and compare natural ester fluid performance to mineral oil, a separate experiment was set up using photo sensors to measure the temperature of the winding and oil. The measuring point of the hot spot temperature was taken to the presumed point due to structural limitation of the winding. Thereafter the hot spot temperature was estimated and compensations were made between the analytical calculation and measurement at the presumed point.

Table 6 shows the temperature results for mineral and natural ester oils using ONAN and ONAF cooling systems for a 154 kV 20 MVA transformer:

Table 6-Mineral oil test results for ONAN and ONAF cooling systems [7]

Mineral Oil Test Results		ONAN Cooling System [°C]			ONAF Cooling System [°C]		
Oil Type	Measurement	Test	Analysis	Error	Test	Analysis	Error
Mineral Oil	Top Oil	56.1	55.0	-1.1	49.9	46.4	-3.5
Mineral Oil	Avg MV	58.9	59.9	+1.0	50.4	49.2	-1.2
Mineral Oil	Avg HV	53.6	55.0	+1.4	44.6	45.5	+0.9
Mineral Oil	Hot Spot (MV)	77.2	75.1	-2.1	64.7	67.2	-2.5

Table 7-Natural ester oil test results for ONAN and ONAF cooling systems [7]

Natural Ester Oil Test Results		ONAN Cooling System [°C]			ONAF Cooling System [°C]		
Oil Type	Measurement	Test	Analysis	Error	Test	Analysis	Error
Ester Oil	Top Oil	63.3	59.2	-3.1	50.5	49.4	-1.1
Ester Oil	Avg MV	61.9	64.2	+2.3	55.5	52.4	-3.1
Ester Oil	Avg HV	58.5	61.2	+2.7	49.7	52.9	+3.2
Ester Oil	Hot Spot (MV)	83.0	84.5	+1.5	78.0	78.7	+0.7

Table 7 shows that when the transformer was filled with natural ester oil, both hot spot temperatures were higher than that of mineral oil. It is observed that the transformer with an ONAN cooling system filled with natural ester oil produced a hot spot temperature of 83 °C making it hottest recorded from measurements. A slight improvement of 5°C is seen when an ONAF cooling system is used.

Bae et al. went on to simulate natural ester oil performance with two transformer design changes:

For the first design, where the winding cooling duct was increased and the radiators were expanded, both electric field and thermal tests were carried out. The insulation system test met the criteria however for an inhomogeneous arrangement a weak point was found at the corner of the windings. A cellulose angle ring was added to strengthen the weak point and the temperature rise test was run with ONAN and ONAF cooling systems. It was seen that the hot spot temperature reduces for an ONAF cooling system. Bae highlights that the hot spot temperatures on windings for an ONAN cooling system is still considerably high and using this design would increase the existing transformer footprint size by 11%.

For the second design, the active part of the transformer was engineered to meet the limitation of existing transformer footprints. Bae et al. decreases the main leg diameter of the magnetic core by utilising high efficient material and further reduces the current densities of the windings. The winding current density is decreased from 4.53 to 4.48 A/mm² to minimize I^2R losses. Furthermore, the radial and vertical dimensions of the winding conductor are adjusted. The radial dimensions of the conductor are increased whilst the vertical dimensions are decreased. To improve the heat radiating efficiency, Bae et al. also increases the vertical winding duct sizes from 5 mm to 7

mm. For this design the height of the radiator fins was also increased as well as more fins were added to improve cooling capabilities. It was seen that the hot spot temperatures dropped significantly for both ONAF and ONAN cooling systems. Both cooling system results can be compared to the performance of mineral oil in Table 4. As a result of this design, they managed to achieve an increased footprint of 0.43% to that of existing transformers.

2.3.2.2 Thermal Design Case Study 2

Frotscher et al. conducted temperature rise tests with two identical transformers filled with mineral and ester oil. The temperature results are displayed in Table 8 below:

Table 8-Comparison of heat run tests for mineral and ester oils using identical transformers [25]

Heat Parameters	Mineral Oil [°C]	Ester Oil [°C]
$\Delta \Theta_{Or}$	59.9	64.4
$\Delta \Theta_{OM}$	46.2	45.5
\mathcal{G}_r	27.4	37.8
$\Delta \Theta_W$	63.4	63.1
Θ_{hr}	82.3	87.3

The observation made during the experiment was that even though the flow rate and velocity is smaller through the cooling ducts, esters contained a better heat coefficient when compared to mineral oil at the same velocity. From the results, Frotscher et al. states that careful considerations should be taken when designing the cooling system of a power transformer. The high viscosity of the natural ester oil created a higher axial winding temperature gradient in the ONAN transformer. For this reason, the cooling ducts for ONAN cooled transformers should be increased to accommodate the higher gradient [25].

2.3.2.3 Thermal Design Case Study 3

In this case study Dombek et al. utilised a finite element software to build a 10 MVA ONAN power transformer model. Dombek et al. ran simulations by inputting parameters for both mineral and natural ester oils and compared the thermal performance. Components such as bushings, control cabinets, conservator tank etc. were removed to simplify the model as it did not affect the thermal efficiency of the transformer [26]. Table 9 shows temperature simulation results (from winding to inner side of tank), Dombek et al. measured for mineral and natural ester oils:

Table 9- Temperature simulation results of mineral and ester oils for a 10 MVA transformer [26]

Distance from winding (m)	Mineral Oil Temperature (°C)	Natural Ester Temperature (°C)
0	65.2	66.3
0.1	62.7	63.4
0.2	62.2	62.7
0.3	62.1	62.7
0.4	62.0	62.6
0.5	61.9	62.5
0.6	61.8	62.4

From Table 9, results show that natural ester oil is slightly hotter than mineral oil. Dombek et al. concludes his research by suggesting that this is still within limits for a 10 MVA transformer but not for larger transformers (160 MVA) as temperature differences between natural ester and mineral oils will be larger. The team recommends that for larger transformers, increasing the size, reducing the load or a modification to the cooling system will assist in lowering temperatures for natural ester oil [26].

2.4. Dielectric Design Considerations

2.4.1. General Considerations for Transformer Insulation Design

When designing the insulation of a transformer it is critical that all factors are considered to ensure total system reliability and optimisation of material. Insulation space impacts the cost of the active parts and influences the quantity of the oil within the unit. These reasons create a competitive global market as companies are constantly focusing on insulation reductions (withstand and operating stress levels) to construct compact and efficient transformers. Advanced simulation computational programs are utilised widely to accurately calculate stress levels which are then compared to established withstand level data [27].

Minimisation of electric stress levels in the insulation design is not the only aspect that must be considered. Other factors in conjunction with electric stresses include:

- Reduction of non-uniform fields
- Creepage stress avoidance
- Impregnation and processing of oil
- Void elimination
- Limitation of high stresses due to winding/transpositions

When analysing the composite-solid insulation system, studies have shown erratic characteristics for mineral oil when used on its own. Observations show that there are large scatters of breakdown voltage for oil when compared to air. These large scatters in mineral oil are normally associated with the random path of streamers and variations. To compensate for these scatters in oil, larger oil ducts are sub divided by solid insulation creating smaller ducts which provides stability to the insulation system [27].

From transformer literature by Kulkarni et al., who analyse insulation design in depth, important test observations can be extracted. They state that the time and frequency of voltage (during power-frequency overvoltage test conditions) is insignificant on creepage strength but is rather more effective on the puncture of solid insulation. The creepage breakdown is more dependent on the failing of the oil when conducting impurities are not present.

For the impulse ratio test conducted on various insulation arrangement types it was shown that the breakdown volt time curve was significantly above the partial discharge volt time curve. Opposite

results were seen for AC long range region test of several minutes as the two curves were closer to each other. Kulkarni et al. deduced that for short times, partial discharge is less effective and will not cause a breakdown of the insulation whereas for durations greater than several minutes it will result in insulation breakdown. It is noted that the 50% breakdown probability voltage is higher for lightning impulses than steep fronted transients.

Another important factor to consider is the Stressed Oil Volume (SOV) effect. It is already known that the breakdown strength in transformer oil reduces as the stress increases for both power frequency and impulse voltages. Designers can choose to either take the stressed volume or stressed area for strength considerations. Generally, calculations are done for stresses in oil. The equation for the breakdown strength in terms of stressed oil volume within an oil gap is given by [27]:

$$E = 17.9(SOV)^{-0.137} \text{ kVrms/mm} \quad (3)$$

Designers must ensure that the calculated stress values are lower than E by some margin. There are two types of electrical failures namely puncture and creepage that must be compensated in the design. For solid insulation, the puncture strength is higher than creepage strength. Maximum creepage strength is only obtained when the equipotential lines are at right angles to the electric field.

An alternative method of calculating the strength of an oil gap can be achieved by cumulative stress calculations. This method also assesses the creepage withstand characteristics. General calculations involve taking the potential difference between two electrodes and dividing by the distance. For more complex systems involving multiple electrodes, the cumulative stress starts at the maximum stress point. The equation for creepage distances for power frequency voltages can be calculated by [27] [28]:

$$E_{creep} = 15d_2^{-0.37} \text{ kVrms/mm} \quad (4)$$

Where d_2 is the creepage path length in mm

The creep strength is usually 30% lower than the bulk oil strength with the withstand curve described by the equation (also known as Weidmann curve) [27] [28] [29]:

$$E_{oil} = 18d_1^{-0.38} \text{ kVrms/mm} \quad (5)$$

Where d_1 is the oil distance in mm between two electrodes

Kulkarni et al. suggest general requirements for designing the insulation system between two windings as seen in Figure 4. Table 10 shows the requirements per area of concern in Figure 4. These considerations do not necessarily apply for ester based insulation systems, but they may be used as a guideline when establishing equations and relationships that describe ester based insulation systems [27]. Design Insulation Level (DIL) is a method used by designers to convert all the standard test voltages (lightning impulse withstand, power frequency withstand) to a design voltage level. Lightning impulse withstand uses a factor of 2.3-2.5 to determine the design voltage level [27] [30].

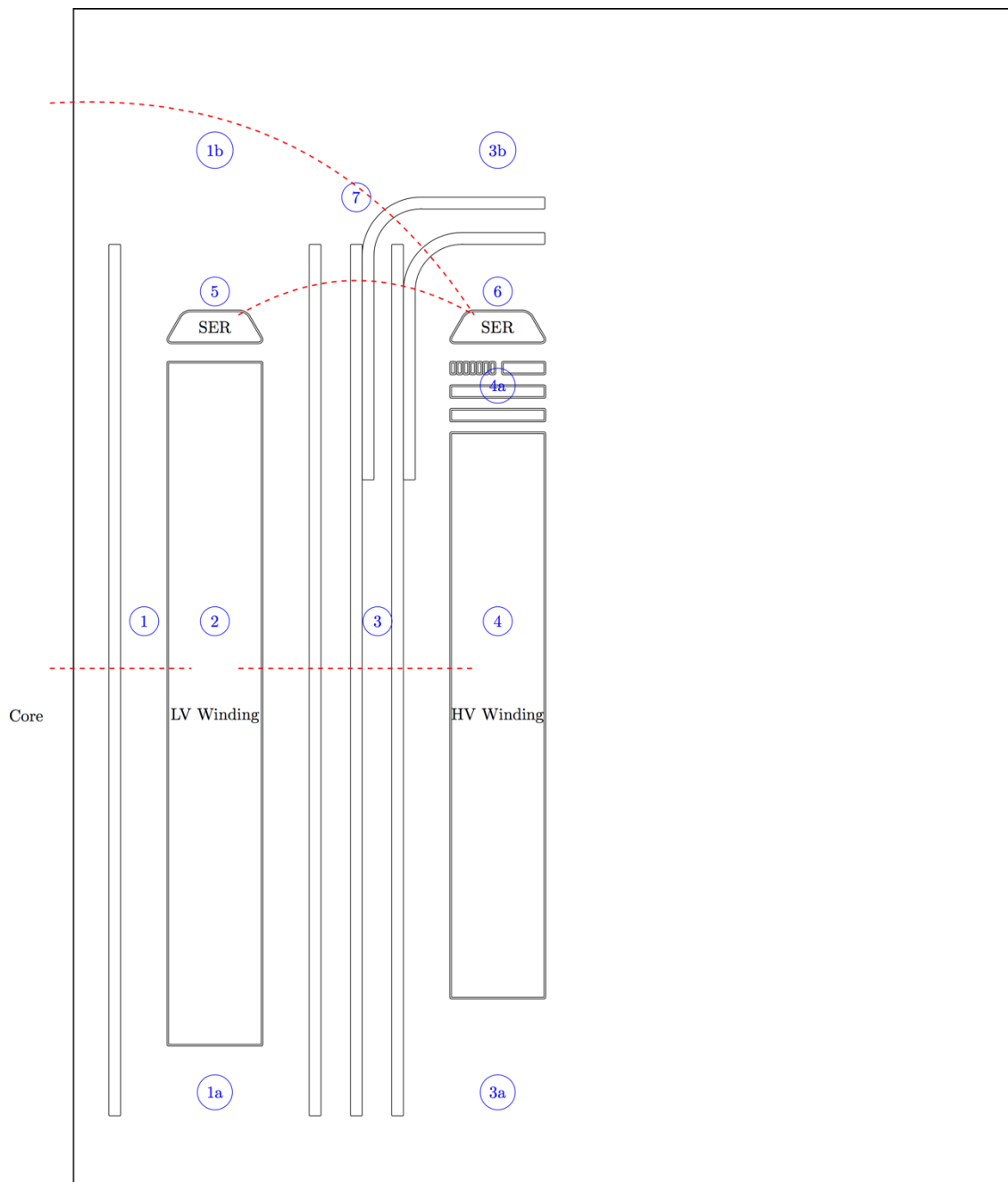


Figure 4-LV/HV Winding Insulation Design Considerations [27]

Table 10- LV/HV Insulation Considerations per Section [27]

Legend	Transformer Design Considerations per Segment
1	<ul style="list-style-type: none"> • Clearance 4.5 - 6 kV/mm for DIL • Less than 8 kV/mm for PD, • Duct size 6-10 mm and pressboard 1.5-3 mm • Apply equation 5 for oil gap strength and equation 4 for creepage strength
1a	<ul style="list-style-type: none"> • Clearance 4.5 - 6 kV/mm for DIL • Less than 8 kV/mm for PD
1b	<ul style="list-style-type: none"> • Adequate space for conductors, pressboard and support • Apply equation 4 and equation 5
2	<ul style="list-style-type: none"> • Paper insulation thickness • Length of winding and grading of field
3	<ul style="list-style-type: none"> • Clearance 4.5 - 6 kV/mm for DIL • Less than 8 kV/mm for PD • First duct size 6-10 mm • Pressboard 1.5-3 mm • Apply equation 5 for oil gap strength and equation 4 for creepage strength
3a	<ul style="list-style-type: none"> • Clearance 4.5 - 6 kV/mm for DIL • Less than 8 kV/mm for PD
3b	<ul style="list-style-type: none"> • Adequate space for conductors, pressboard and support • Apply equation 4 and equation 5
4	<ul style="list-style-type: none"> • Paper insulation thickness • Length of winding and grading of field
4a	<ul style="list-style-type: none"> • Field must be checked between the layers and at the edges of the conductors
5	<ul style="list-style-type: none"> • Graded field
6	<ul style="list-style-type: none"> • Paper insulation 2-3 mm • Radius approximately 2mm and 6mm for bottom and top respectively
7	<ul style="list-style-type: none"> • Angle rings are used to subdivide the oil gaps (shaped according to equipotential lines) • Apply equation 5 for oil gap strength and equation 4 for creepage strength

2.5. Considerations for Ester Design

The following section reviews characteristics that focus on the design perspective of transformers with natural ester oils.

2.5.1 Relative Permittivity

Edison investigated the permittivities for both mineral and ester oils against temperature [31]. They further investigated the permittivities for kraft paper impregnated with mineral and ester oil. Their tests show that natural ester oil contains a much higher permittivity than mineral oil and this is retained even when impregnated with kraft paper. The typical permittivity of ester fluid is approximately 3.2 which is closer to the permittivity of kraft paper (approximately 4.4). This finding from their tests showed to have a capacitive effect on the dielectric design. However, Darwin et al. proved that even though the capacitance of the insulation structure changes, it was not significant for impulse applications [5]. Prevost et al. concluded from his tests, that the electrical stress in the solid/liquid insulation system will distribute inversely proportionally to the permittivities of the respective fluids [6]. He also found that the electrical stress was concentrated more in the solid insulation than the natural ester fluid and stated that bringing the permittivity closer together means that the stress is distributed more evenly between the fluid and the solid material, which effectively reduce the gap spacing required. [6]

2.5.2 Breakdown Voltage

Darwin et al. compare different insulating fluids namely mineral, synthetic and natural ester oils and derive fundamental characteristics for each type. Breakdown voltage tests were done in accordance to the IEC 60156 standard (spherical electrodes with 2.5 mm gap). For 6 mean measurements it was observed that both natural and synthetic esters displayed BDV greater than 70 kV, which was similar to mineral oil [5]. The Cigre workgroup for new insulating fluids discuss multiple tests for both natural ester and mineral oil. Their results were similar to Darwin et al. findings [24].

2.5.3 Streamer and Long Gap Breakdown of Natural Ester Fluid

Rapp et al. conduct both AC and lightning impulse tests (500 kV) for ester and mineral oil filled transformers in a slightly non homogeneous system. For both tests, the team focuses on long oil gaps found between the bushing shield and tank which forms part of the critical insulation design of a power transformer. Gaps of 50, 100, 125 and 150 mm were tested by raising the bushing height used for the applied voltage [32]. These 60 Hz tests were conducted in accordance with IEC 60060-1. Results showed that natural esters displayed a lower AC breakdown and withstand than mineral oil at the start (50 mm) but at the 100 mm gap mark had converged and began surpassing mineral oil [32]. They conclude that for both positive and negative polarities, natural ester oil is closely comparable to mineral oil [32] for slightly non homogenous fields

Duy et al. conduct investigations on streamer propagation in natural esters and mineral oil. The experiments were carried over gap lengths between 2-200 mm and voltages up to 460 kV [33]. Analysis of slow (velocity of 1 km/s) and fast (velocity of 200 km/s) streamer propagation under high impulse voltage ranges utilising the point to plane electrode system was carried out.

Duy et al. uses the point to plane electrode system with a 100 mm gap and conducts tests by varying the electrode voltage from 140 kV to 241 kV. Comparisons with mineral oil show that esters induce streamers more easily for both polarities and at lower breakdown voltages. In natural esters, positive streamer propagation evolves much rapidly from a slow streamer to fast streamer under high voltages. This is not the case for mineral oil which shows better stability in these conditions. In large gaps the existence of fast streamers induces a low tolerance to short duration transients such as lightning impulses and must be considered when designing the insulation system of a natural ester transformer [33].

Lui et al. conduct experimental studies on streamer formation and breakdown in ester oil with a pressboard interface. Both positive and negative polarities are tested under lightning impulse conditions utilising a divergent point to plane field arrangement. From pre-breakdown experiments, it was observed that streamers on the ester/pressboard interface represented similar characteristics as streamers in open gaps and had no effect on the stopping length. Under negative polarity specifically, streamers on the ester/pressboard interface propagated further than the mineral oil/pressboard interface under the same voltage.

For the ester/pressboard interface, breakdown voltage was found to be lower than mineral oil/pressboard. This difference was magnified at larger gap sizes. Lui et al. noticed that pressboard

surface damage was more noticeable on the mineral oil/pressboard interface than ester/pressboard interface after breakdown conditions for negative polarity [34].

For overstressed positive polarity conditions, the introduction of pressboard interface shows significant reduction of acceleration voltage in mineral oil however surface damage is more evident. For overstressed negative polarity conditions, both ester and mineral oil in the presence of pressboard accelerates the streamer velocity at larger gap distances and higher voltages. In conclusion Lui et al. establishes that the acceleration voltage is much lower for ester/pressboard interface which makes this system more susceptible to fast streamers [34].

2.5.4. Cumulative Creep

When designing a dielectric system, it is critical to ensure that the stress along the solid/liquid insulation interface is within acceptable limits. Even though most insulation systems utilise contoured components there still exists interfacial and creep stresses along the surface. Electrical stresses in the form of equipotential lines are found in most power transformers. When these equipotential lines cross any part of the solid insulation, a voltage differential is created forming a dielectric stress tangential to the solid insulation surface. Weidmann developed a curve utilising kraft pressboard for mineral oil. The curve provides limits for cumulative stress calculated tangentially along the solid/liquid interface and is based on a 1% probability of partial discharge interception [6] [31]. Both Cooper industries and Prevost et al. used the high voltage electrode test to examine the behaviour of natural ester fluid. This experiment consists of a U shaped copper or brass tube which is covered with kraft paper insulation. A block of laminated pressboard is placed between the paper insulation and a metallic ground electrode. The pressboard exhibits the creep stress when AC and negative impulses are applied. The results from Cooper industries and Prevost et al. indicate that the creep strength, utilising natural ester oil, of pressboard is equivalent or even better than mineral oil for AC and negative impulses [6] [31].

2.5.5. Dielectric Design Case Studies

2.5.5.1 Dielectric Design Case Study 1

Fritsche et al. present their work on a 420 kV 300 MVA FR3 fluid transformer manufactured by Siemens which was put in operation in 2014. They discuss the physical, electrical and chemical design aspects of this transformer.

Physical Aspects: Since FR3 fluid contains a higher viscosity than conventional mineral oil, they recommend that the configuration and winding arrangement be modified. Oil ducts should be increased when compared to mineral oil ducts to limit the pressure drop along the winding. Fritsche et al. states that a higher kinematic viscosity can benefit aging in the paper as natural ester oils contain superior specific heat capacities and thermal conductivities which allows for more energy to be transferred from the windings [3] .

Electrical Design Aspects: Fritsche et al. illustrate the breakdown voltage behaviour for an inhomogeneous point to plate arrangement with different insulating fluids. Special tests were carried out by the team to evaluate and verify the dielectric strength for AC (630 kV), LI (1425 kV) and SI (1050 kV) conditions. The observation made by the team was that when the electrode distances were increased, the related breakdown voltage ratio for both mineral oil and ester oil increased [3]. They showed that clearances between the windings and grounded elements need to be adjusted accordingly with factors of 1.2 – 1.4 for esters. Fritsche et al. also considers modifying the insulation design of the oil ducts within the barriers at the winding end. They further suggest that long oil gap distances should be sub divided by special insulation barrier boards. This is done to avoid the breakdown of the oil gap under AC or LI stresses.

2.5.5.2 Dielectric Design Case Study 2

Marchesan et al. from WEG T&D in Brazil, present their study of two ester power transformers in the voltage class of 69 kV and 245 kV with maximum BILs of 1300 kV. The study focuses on the dielectric characteristics of natural ester fluids in non-uniform electric fields and long gap distances. Marchesan et al. carries out electric field winding simulations for both natural ester and mineral oil.

It was observed that the voltage stresses increase in the paper insulation for natural ester oil when compared to mineral oil which correlates to the findings of Prevost et al. This can be seen as

beneficial as there is less stress in the oil due to the difference in dielectric constants of the material. Impulse voltage tests on the 69 kV prototype transformer (designed to mineral oil specification), filled with natural ester oil, were also carried out with three phases consisting of the same dielectric distances and composition between solid and liquid insulation. The experiment used the rising voltage method used for dielectric tests which increases the BIL voltage by 5% per measurement. For each test, three full and two chopped voltage waves were applied. The results from the impulse test produced the following:

- Phase A – At 100% of the design BIL, failed at the first full wave impulse wave
- Phase B – Passed all tests at 100% of the design BIL, but failed at the first full wave applied at 110%
- Phase C – Passed all chopped waves at 110% of the design BIL, but failed at the second full wave applied at 100%

Marchesan et al. repaired the prototype and made changes only to phase B. The adjustments made were not detailed in the paper. A retest using a modified phase B produced an approved 130% of the design BIL. Marchesan et al. tests highlight the importance of dielectric design modifications needed when using natural ester oil.

For the second test, Marchesan et al. makes use of a 245 kV single phase transformer (designed to mineral oil specification) to determine the probability of discharge in natural ester oil. Finite element analysis was performed to determine areas of discharge on the winding. The simulation results correlated to the laboratory experiment and showed that the long gap discharge path of failure occurs (at 100% BIL) at the center of HV winding when designed according to mineral oil insulation parameters.

Marchesan et al. concludes from his experiments that discharge takes place for creep distances higher than 150 mm in natural ester oil. When a high intensity non uniform electric field is able to produce the inception for discharge in natural ester oil, it propagates at a higher velocity than mineral oil. This is a major disadvantage as high propagation velocities reduce the dielectric system within the transformer [1].

2.5.5.3 Dielectric Design Case Study 3

In this case study, Frotscher et al. conduct numerous tests and analyse the dielectric behaviour of natural ester oil [25]. Their experiments show similar characteristics for homogeneous and inhomogeneous configurations.

Frotscher et al. observe that gas bubbles remain longer in natural ester oil than mineral oil due to its higher viscosity. This poses a problem for ester oil as formation of micro bubbles will initiate local discharges more easily than mineral oil. This will abet oil breakdown which could lead to a transformer failure. The streamers phenomenon is also analysed in depth.

Frotscher et al. conducts oils tests and from the results, esters displayed a much lower voltage for both negative and positive polarity impulse voltages implying that streamers are developed at much lower voltages in ester when compared to mineral oil. Fast streamers were concentrated and stronger in positive polarity voltages than in the negative polarity. These fast streamers contained longer L_s values which is a major disadvantage as breakdowns can occur over long oil gap distances. Froscher et al. found that both mineral and ester oils possess similar inception voltages [25].

Due to the permittivity of natural ester oil being 40% greater than mineral oil, Froscher et al. examines the electric field distribution within the windings. He observed that the permittivity ratio between paper and the oil is lower for esters than mineral oil. This creates lower electric field strengths in the oil for esters. On the other hand, electric field strengths are more concentrated in solid insulation for ester oils when compared to mineral oil [25].

Field calculations from the FEM model show that the electric strength is approximately 8% lower for ester oil. It is noted that even though solid insulation materials possess higher dielectric strengths than liquids, there are no negative effects for both homogenous and marginally inhomogeneous arrangements. For full inhomogeneous systems, caution must be taken for existing paper insulation limit values as the higher electric field strengths can exceed the design. Frotscher et al. highlights two advantages of ester oil over mineral oil namely:

- A more homogenous electric field strength distribution is present for combined solid and liquid insulation systems
- There is a reduction in field strength within the oil ducts

Frotscher et al. concludes that for an ester inhomogeneous system with uncoated components, fast streamer discharges would be a major problem for existing designs. The team suggests that existing

designs should be modified to compensate for longer insulation gaps and additional barriers to counter these effects. The team confirms that all commonly used transformer material can still be incorporated when using ester oil. Due to the high viscosity, thick insulation elements will require additional bored holes so that impregnation is improved and ester oils are required to be filled at higher temperatures (20°C higher) especially on transformers carrying a low load [25].

2.6 Summary

Table 11 consolidates all design recommendations made for a full natural ester transformer.

Table 11-Summary of Thermal and Dielectric Design Considerations for Natural Ester Oil

Design Consideration	Thermal	Dielectric
Permittivity	-	Ensure close matching of permittivities for natural ester oil and insulating material
Viscosity	Increase duct sizing Alter the dimensions of the external radiators or add more fins to the existing design Increase oil impregnation times for paper	-
Creepage	-	Ensure electric field stresses along solid/liquid insulation interfaces are within acceptable limits
Streamers	-	Increase clearances between different potentials, insert more insulation barrier and avoid inhomogeneous systems

3 Transformer and Winding Design

The following section covers the basic design of the 88 / 6.6 kV 20 MVA transformer, which has been validated against local manufacturers.

3.1 Winding Arrangement

The transformer consisted of the LV winding, HV winding and the tap winding wound around the core limb as illustrated in Figure 5. The tap winding was excluded in this study as the focus was the design changes between mineral and ester oil.

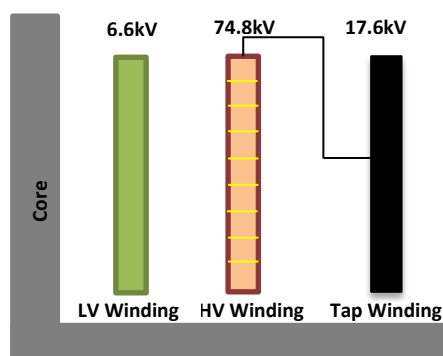


Figure 5- Winding configuration

3.2 HV and LV Winding Phase Currents

The phase currents for windings are calculated by the following equation [27]:

$$I_{HV(\text{phase})} = \frac{20\text{MVA}}{\sqrt{3} \times HV} \quad (6)$$

For the nominal voltage of 88 kV, the phase current would be 131 A. For the LV winding, the line current would be 1752 A while the phase current would be 1012 A.

3.3 Core Dimensions and Volts per Turn

To determine the dimensions of the windings the core diameter and limb area must be calculated. The core diameter equation is given by an empirical expression [27]:

$$\text{Core } \phi = 40 \sqrt[4]{kVA} \quad (7)$$

The limb area is given by [27]:

$$\text{Limb Area} = \frac{\pi d^2}{4} \times 0.84 \quad (8)$$

Where the factor of 0.84 is the fill factor for the core and is the ratio between the magnetic and non-magnetic core material.

The volts per turn are given by equation [27]:

$$V_{\text{turn}} = 4.44 \times B \times \text{Area}_{\text{core}} \times f \quad (9)$$

Where B is the design flux of the transformer and was 1.7 T in this case.

The number of turns is based on the volts per turn and is given by [27]:

$$N = V_{\text{phase}} / V_{\text{turn}} \quad (10)$$

Table 12 has the core and winding information used for this study.

Table 12-Winding and Core Properties

Parameter	Value
Core diameter	475.5 mm
Limb area	0.125 m ²
Volt per turn	56
Primary turns (HV winding)	902
Secondary turns (LV winding)	117

3.4 Winding Design

To design the windings, the core dimensions and the core window height and width dictate the dimensions of the winding. In addition, the manufacturer's capability would influence the design of the winding. The winding dimension would also need to consider the dielectric clearances as well as the need for cooling ducts. In Figure 6, WH refers to the winding height while CH refers to the window height. The required gaps between the windings are shown. The gaps between the top and bottom of the windings would also need to be considered.

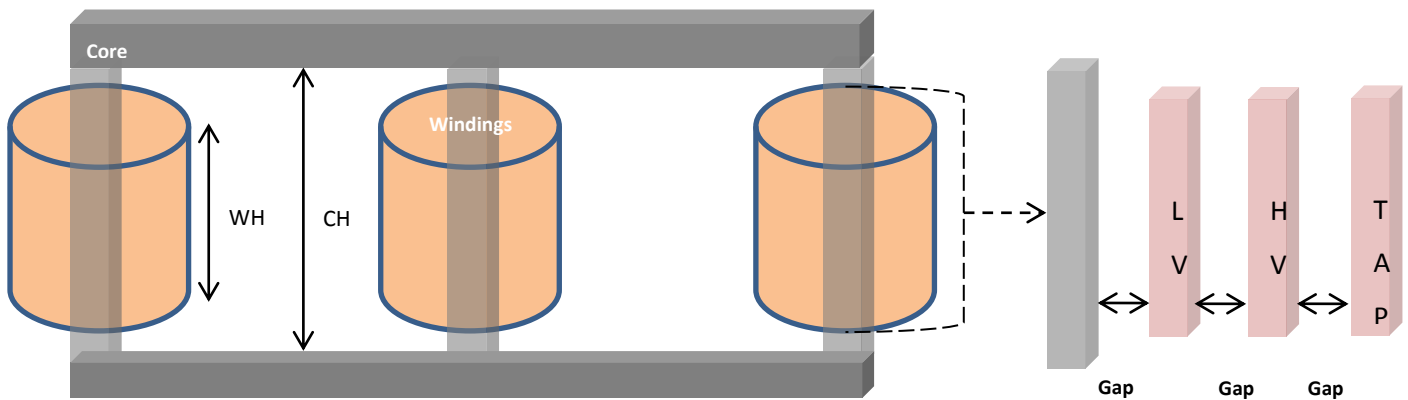


Figure 6 - Winding layout showing

3.4.1 Dielectric Clearances

The typical design insulating levels (DIL) required for calculating the winding dielectric parameters are given by the following equation [30]:

$$DIL = \frac{BIL}{\text{Factor}} \quad (11)$$

Manufacturers use factors varying between 1.9 and 2.8 depending on the factory capabilities. Kulkarni uses 2.3 to determine the design insulation level [27]. In this study, a factor of 2.65 has been used [30]. Electric utilities typically allow up to 5.7 kV/mm for electric gap stresses (E_{design}),

this value depends on capabilities of the manufacturer. This value has been used to calculate the minimum clearances.

$$Clearance = \frac{DIL}{E_{design}} \quad (12)$$

Table 13- Electrical Properties for Winding and Core

Gap	Power Frequency Withstand	BIL	DIL	Minimum Clearance	Comment
Core – LV	22 kV	75 kV	28 kV	4.97 mm	Needs to account for cooling ducts
Core – HV	95 kV	380 kV	143 kV	25.16 mm	Needs to account for cooling ducts, any leads and static electric ring
LV – HV	95 kV	380 kV	143 kV	25.16 mm	Needs to account for cooling ducts

Table 13 shows the specified BIL between the core and windings. Considering the Weidmann curve from Equation 5, a clearance of 25.13 mm has a withstand stress of 5.29 kV/mm, this is below the design stress of 5.7 kV/mm. The division of the clearance between the LV-HV windings due to the cooling ducts would divide this. Selecting a duct spacing of 10 mm next to both the LV and HV windings (as in Figure 4 and Table 10), the withstand stress would be increased to 7.5 kV/mm. The design stress is well below this.

3.4.2 LV Winding Dimensions

The type of winding considered in this study is the disc type winding. A design current density of 3 A/mm² is used. The minimum conductor cross-section area is given by [9] [27]:

$$A = \frac{I}{J} \quad (13)$$

The cross-sectional area required is 337 mm². The conductors would be arranged in parallel as shown in Figure 7, to achieve the required cross-sectional area.

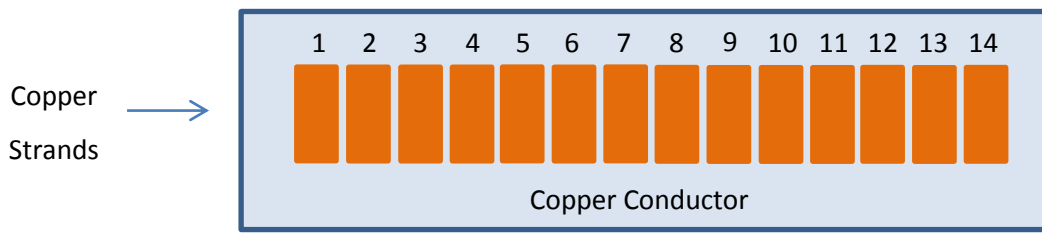


Figure 7-LV conductor strand layout

The core window height has been assumed to be 1500 mm, and the height of the winding is 1350 mm (or 90% window height), considering spacers of thickness of 2 mm and a total number of turns as 117, the disc thickness is approximated by:

$$T_{disc} = \frac{WH}{N} - t_{spacer} \quad (14)$$

After determining the thickness of each disc, the width of the winding can be determined. Note that the values are increased by 0.5 mm to account for the paper covering. A further 10 mm should be added to the winding to account for a cooling duct in the centre of the winding. The final LV conductor, core clearance and winding disc properties is seen in Table 14

Table 14- LV Conductor, Core Clearance and Winding Disc Properties

Parameter	Value	Comment
Winding height	1350 mm	-
Min conductor cross-sectional area	337 mm ²	-
Disc thickness	10 mm	-
Disc width	46 mm	Includes cooling duct of 10 mm
Number of discs	117	-
Clearance Core-LV	15 mm	Includes cooling duct of 10 mm
Electric stress for Core-LV Gap	1.89 kV/mm	-

3.4.3 HV Winding Dimensions

A similar approach is used for the HV winding, the type of winding considered was also the disc type winding. A design current density of 3.5 A/mm² is used. The number of turns is greater and the cross-sectional area is less. In this case it was assumed that the number of discs were the same on the HV as the LV. The thickness was calculated using the equation above but with a spacer thickness of 3 mm. The disc width was approximated by:

$$W_{disc} = \frac{N}{N_{disc}} \times \text{Conductor width} \quad (15)$$

The final HV conductor, core clearance and winding disc properties is shown in Table 15.

Table 15-HV Conductor, Core Clearance and Winding Disc Properties

Parameter	Value	Comment
Winding height	1350 mm	-
Min conductor cross-sectional area	37.5 mm ²	-
Disc thickness	9.5 mm	Includes insulation of 0.5 mm
Conductor thickness	9 mm	-
Conductor width	4.2 mm	Excludes insulation of 0.5 mm
Disc width	46 mm	Includes cooling duct of 10 mm
Number of discs	117	-
Clearance Core-HV	75 mm	-
Electric stress for Core-HV Gap	1.9 kV/mm	-
Clearance LV-HV	30 mm	Includes 2 pressboards of 2 mm thickness
Electric stress for LV-HV Gap	4.8 kV/mm	-

4. Simulation and Results

4.1. Dielectric Simulation using FEM Model

Chakraborty et al. analysed a power transformer using FEM. They used the simulation package ELECTRO. It was difficult to understand where they had plotted and what their main results is as they did not relate the electric field to the relevant design margins [35].

Ziomak et al. [29] presented their design criteria and a number of examples in FEA. The criteria they are looking for are:

- The maximum local stress at the surface of the insulated or un-insulated electrode, which they state must be below 11-12 kV/mm,
- The stress along the oil gaps, which must be less than the Weidmann curve
- The creepage stress along solid insulation, which must be less than the creep stress curve.

One of the objectives for this research is to develop a power transformer model in FEM and use it to determine the dielectric characteristics of an ester oil based 88/6.6 kV 20 MVA power transformer. It is critical to confirm that ester oil is within calculated dielectric limits this transformer. Some important dielectric areas to analyse for using ester oil include the stresses between windings, paper, pressboard and the oil itself. The model was developed based on the general considerations in Section 2.4.1. It is understood that these rules may be different for ester based transformers and that the physical dimensions may be differ due to thermal considerations. FEM is a numeric process of quantifying energy principles or governing differential equations into a system matrix for approximate solutions. This method entails taking the application domain and dividing it into sub domains called finite elements. These sub domains are independently solved to find a complete solution [36].

Figure 8 below shows the flowchart representing rules used to design the insulation system for the 88kV dielectric simulation:

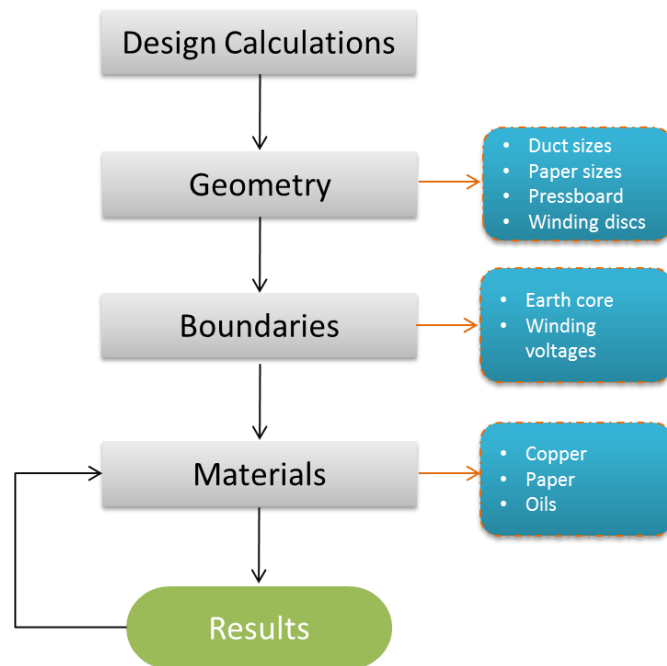


Figure 8-Flowchart of insulation system design for dielectric simulations

An explanation of the above flowchart is described in the following steps:

Step 1 – Design Calculations

A generic power transformer insulation system is designed from first principles based on the considerations in Section 2. The section of the transformer consisted of the core, LV winding and HV winding of 6.6 kV and 88 kV respectively. These voltage levels correspond to BIL of 75 kV and 380 kV respectively, or DIL of 33 kV and 165 kV [27]. Assuming a cumulative electric field of 5.7 kV/mm the minimum gap between the core and LV winding is 5.7 mm, and between the LV winding and the HV winding is 29 mm. The model further accounted for pressboard of thickness 2 mm and cooling ducts of 10 mm next to the windings

Step 2- Geometry

The geometry is made up of core, LV and HV windings that are represented by simple rectangular blocks with parameters from the calculated design. All the components are drawn in the software program Femm 4.2 which is CAD based.

For this dissertation a pair of windings was simulated as seen in Figure 9:

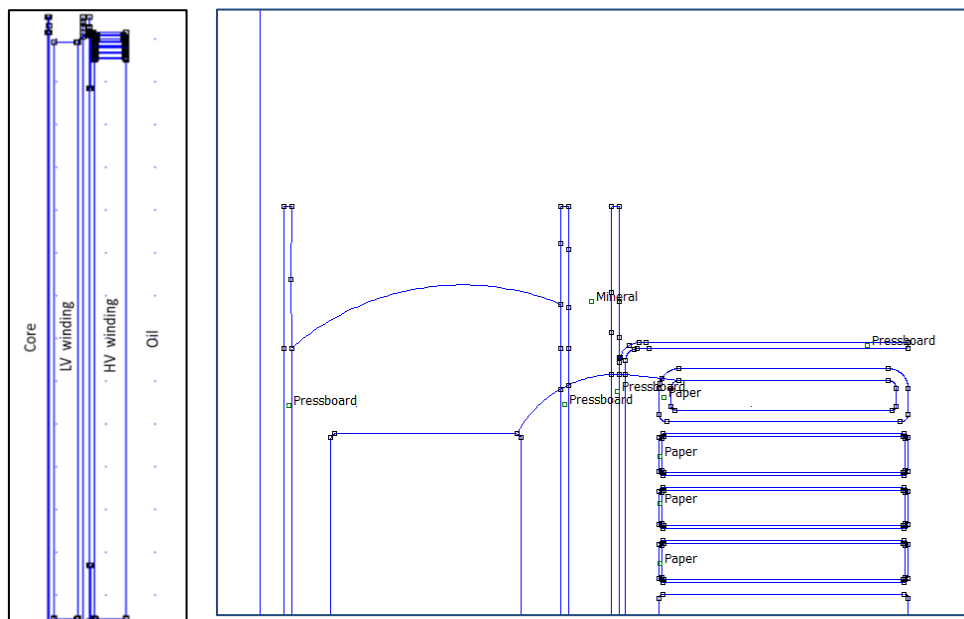


Figure 9-Flowchart of insulation system design for dielectric simulations

Figure 9 shows a detailed top section of the Core/LV/HV winding interface. For simulation purposes the HV winding is broken up into a stress control ring and four winding discs covered with kraft paper. Stress-control rings serve two functions of reducing the electric field strength and it influences the initial voltage distribution on the HV winding [36]. Pressboard has been inserted for winding insulation as well as oil duct formation. This common configuration of an LV/HV winding has been closely built according to design principles in Section 2.4.1 [27]. These include clearances between core/HV/LV windings, spacers and paper thickness. Once the geometry has been setup, it is divided into finite elements. A mesh with multiple nodes is applied to the geometry which provides a higher accuracy to the results, seen in Figure 10.

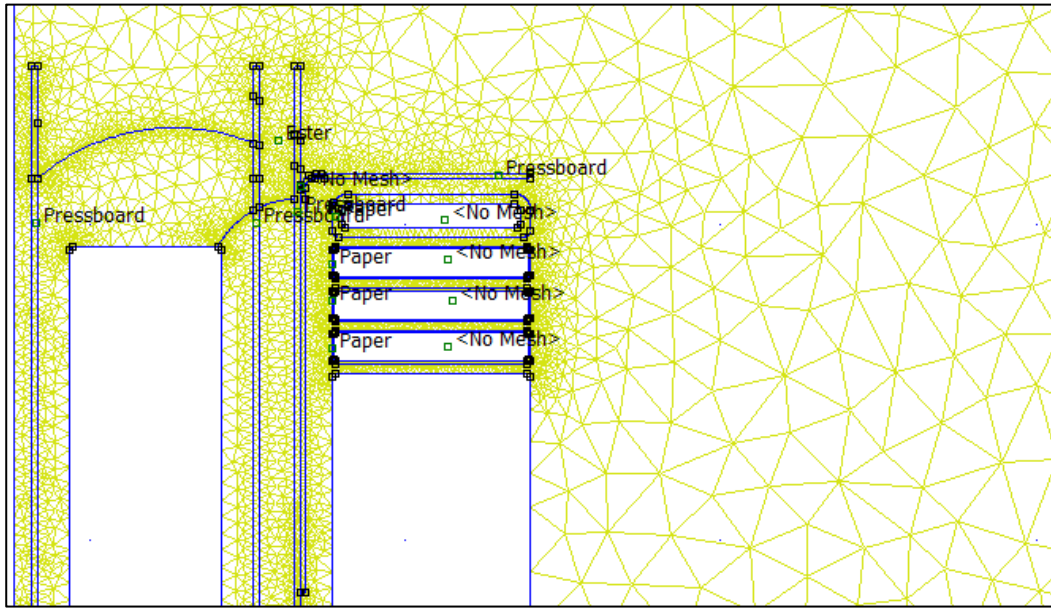


Figure 10-Transformer geometry with mesh applied

Step 3 and 4- Boundaries and Materials

After inputting parameters, FEM will calculate the electric field in the transformer and will represent the worst case conditions for the insulation structure. Therefore, the chosen boundary conditions might or could not describe the problem exactly as it is in real transformer. The Neumann boundary condition, $\frac{\partial V}{\partial n} = 0$ [36], was chosen for this model as it provided the highest electric field. This boundary condition was applied on the right side of the model as the electric field is symmetric to the mid-plane of the HV windings. The left side of the LV winding in this case is earth which represents the core of a transformer. The core has a relatively high permeability and does not store any significant energy. For the simulation, earth was set to zero voltage shown in Figure 11.

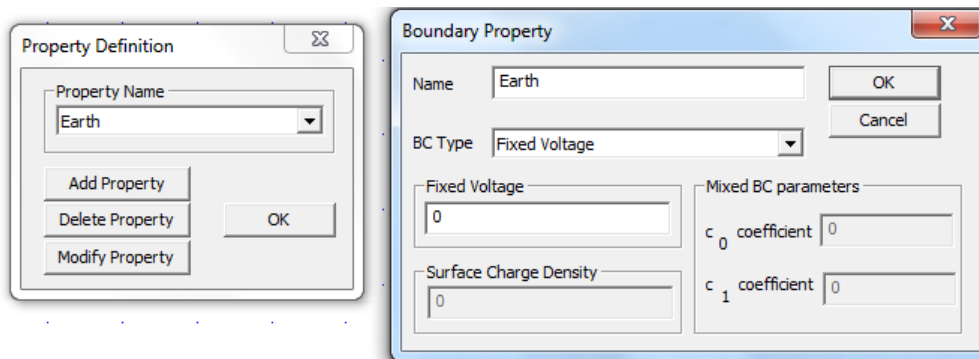


Figure 11-Boundary- Earth set to zero voltage

The four materials that make up the dielectric model are ester oil, mineral oil, kraft paper and pressboard. Each material contains its own permittivity which was entered into the model as seen in Figure 12.

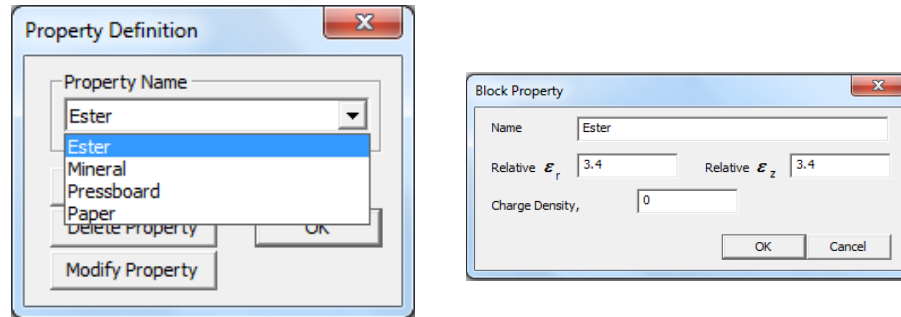


Figure 12-Ester oil assigned a permittivity

Typical permittivities per material are shown in Table 16. This was entered into the Femm software package as seen in Figure 13

Table 16-Relative permittivities considered for the insulation design

Material	Relative Permittivity (F/M)
Paper	2.8
Ester Oil	3.4
Mineral Oil	2.2
Pressboard	4.4

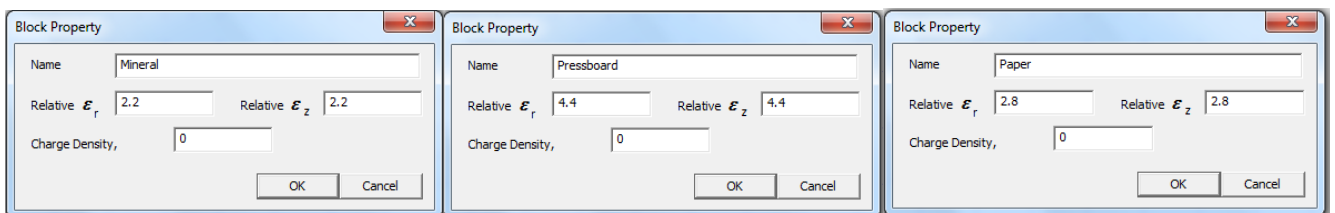


Figure 13-Assigned permittivity per material

4.1.1. Results

Eleven dielectric simulations were carried for this research with each containing a different possible path. To evaluate the dielectric behaviour of both oils, individual paths are drawn in FEM (red line) per simulation which include the following areas of concern:

- HV to LV winding (Top section)
- HV winding to Core
- HV to LV winding (Middle section)
- HV to LV winding (Bottom section)
- HV to HV winding (between discs)

Since natural ester oil has a density and viscosity that is different to mineral oil, more insulation intensive designs are required. Marchesan [1] and Prevost [6] had previously concluded via tests that for natural ester oil the electrical stresses are present in the paper as opposed to mineral oil where the stresses are in the oil.

4.1.1.1 Simulation 1

Figure 14 illustrates electric field images for mineral oil and the ester respectively. The same scale was used for colour mapping so that both mineral and ester oil fields could be directly compared. In this case the electric field is investigated around the expected highest field from the top of the HV winding (static electric ring) to the LV winding.

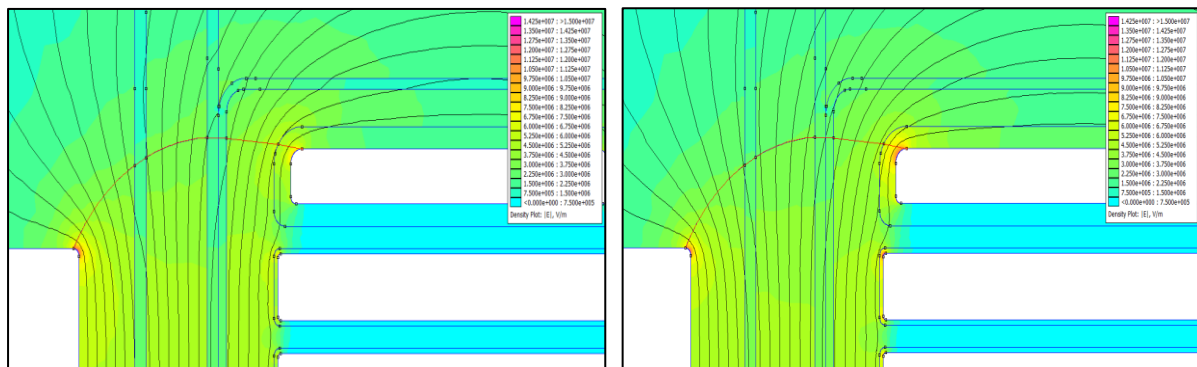


Figure 14- (left) Mineral Oil-HV to LV winding path-Top section; (right) Ester Oil-HV to LV winding path-Top section

This is due to the higher permittivity of natural ester oil, which is closer to that of kraft paper than mineral oil [6].

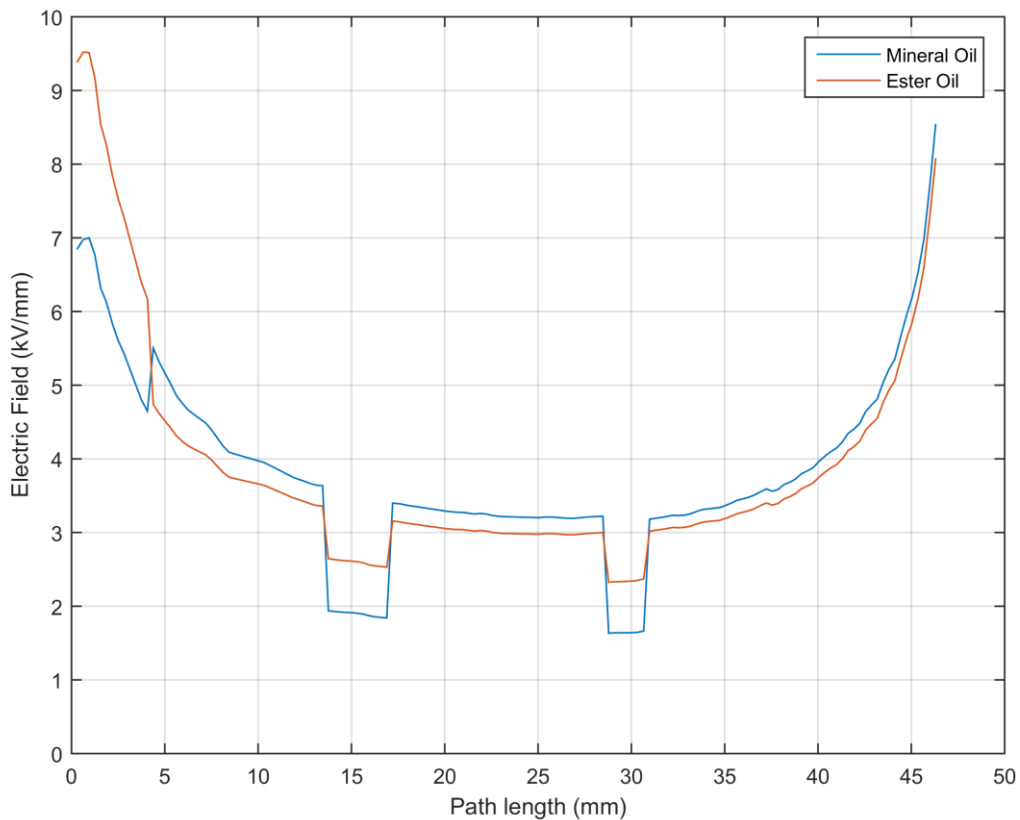


Figure 15-Electric field vs Path Length for mineral and ester oils (HV to LV winding path)

Figure 15 shows both mineral oil and ester oil dielectric stresses plotted against each other. At the HV winding initial start path (represents paper), it is seen that the stresses in natural ester oil are much higher when compared to mineral oil. As the path length increases from 0 to 10 mm (represents oil), the stresses reduce for natural ester oil which drops below mineral oil. Between 13 mm to 16 mm (represents pressboard), stresses are concentrated more for natural ester oil than mineral oil due to similar permittivities of pressboard. This sequence continues until the simulation path eventually reaches the LV winding.

4.1.1.2 Simulation 2

The electric field between the LV and HV winding (middle section) is illustrated in Figure 16 for mineral oil and ester oil respectively.

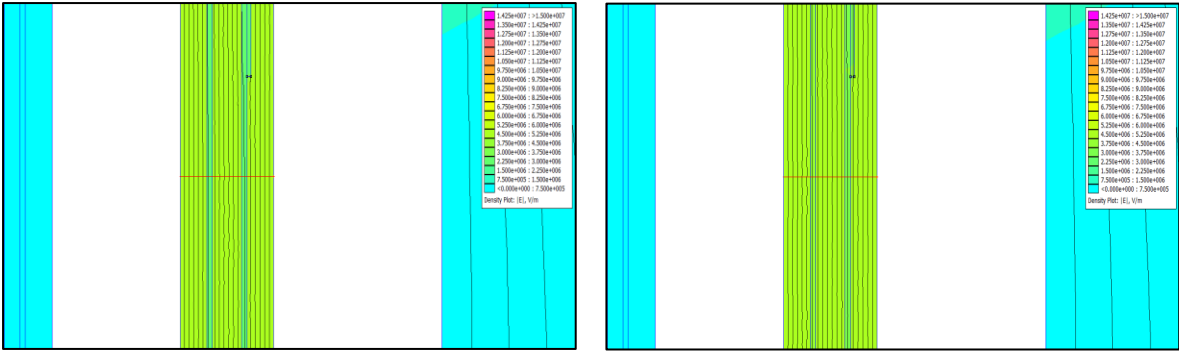


Figure 16-(left) Mineral Oil-HV to LV winding path-Middle section; (right) Ester Oil-HV to LV winding path-Middle section

The dielectric behaviour is similar to simulation 1 for the shortest distance (mid-section) between the HV and LV winding. Once again it is seen that stresses are higher (in oil) for mineral oil than natural ester oil and are prominently less in pressboard. However, a significant difference can be seen in Figure 17 at the initial starting point of the simulation (0 mm), as the total stresses of the HV winding is measured to be below 5 kV/mm when compared to 9.3 kV/mm in Figure 15.

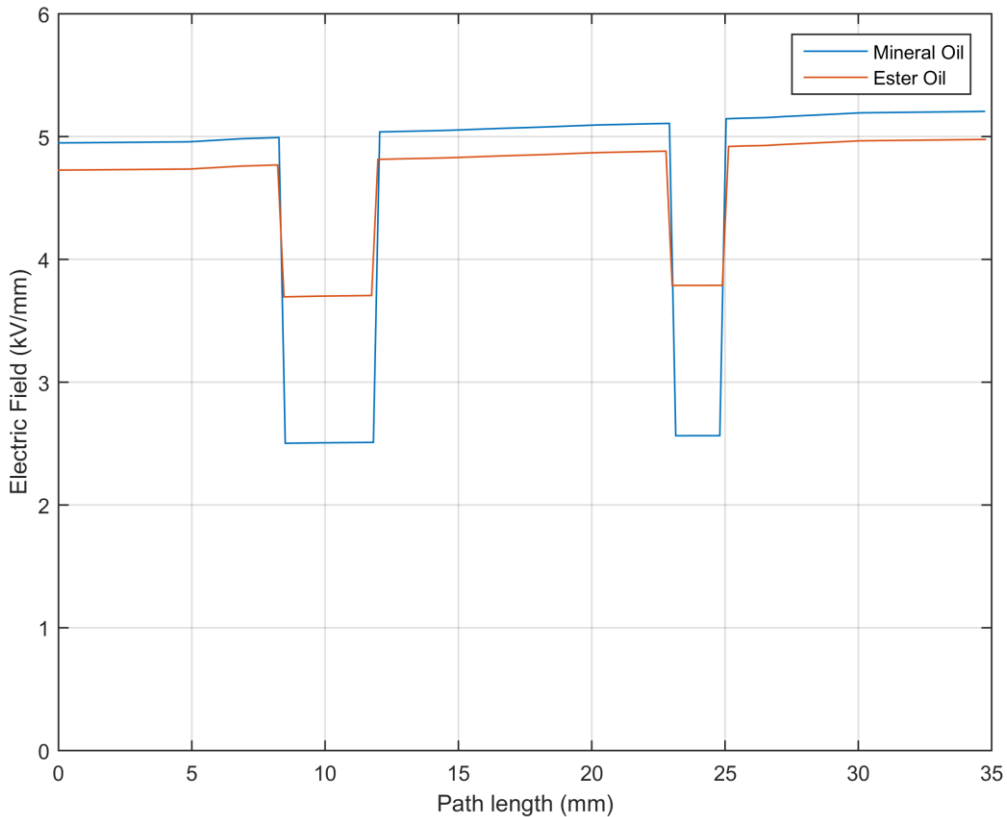


Figure 17-Electric field vs Path Length for mineral and ester oils (HV to LV winding path)

Since higher stresses are contained in the paper for natural esters, increased paper insulation is a necessity for these types of transformers. For these applications, thermally upgraded kraft paper will be a recommended option to use around the winding conductor as it is thicker and contains a higher permittivity than standard insulation paper. To simulate thermally upgraded kraft paper in the model, the relative permittivity of the paper was adjusted to 3.5 (typical entry level for thermal upgraded paper). The path chosen, seen in Figure 18, was from the top section of the HV winding to the LV winding. The model was run again and the results in Figure 19 showed that the stresses were drastically reduced in the paper of the HV winding for natural ester oil.

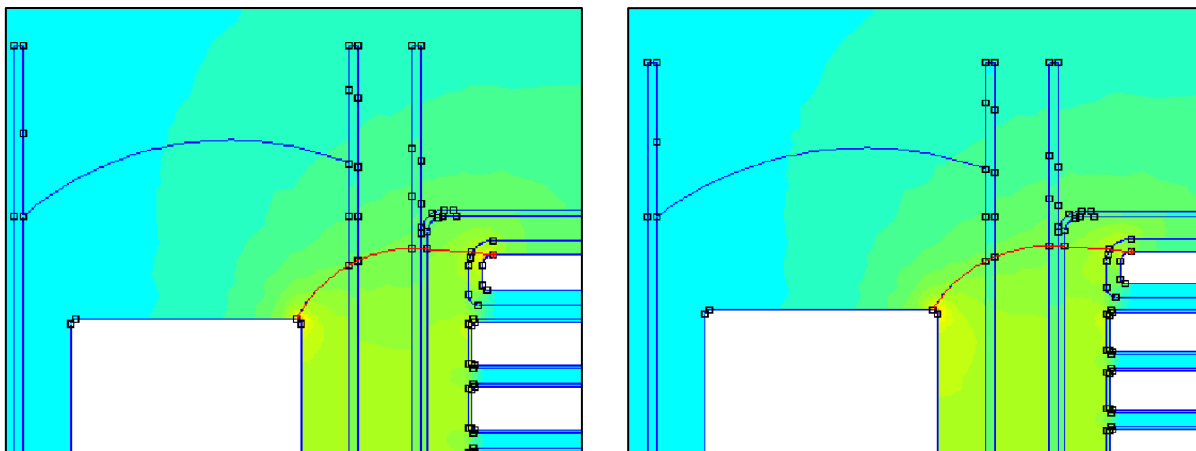


Figure 18-(left) Mineral Oil dielectric stresses with thermally upgraded kraft paper; (right) Ester Oil dielectric stresses with thermally upgraded kraft paper

Mineral oil displays no stress change from the results and remains the same as seen in the above figure. A comparison between the electric field vs path length graphs for standard kraft and thermally upgraded kraft paper shows almost a 1 kV/mm reduction in the paper as seen in the figure below.

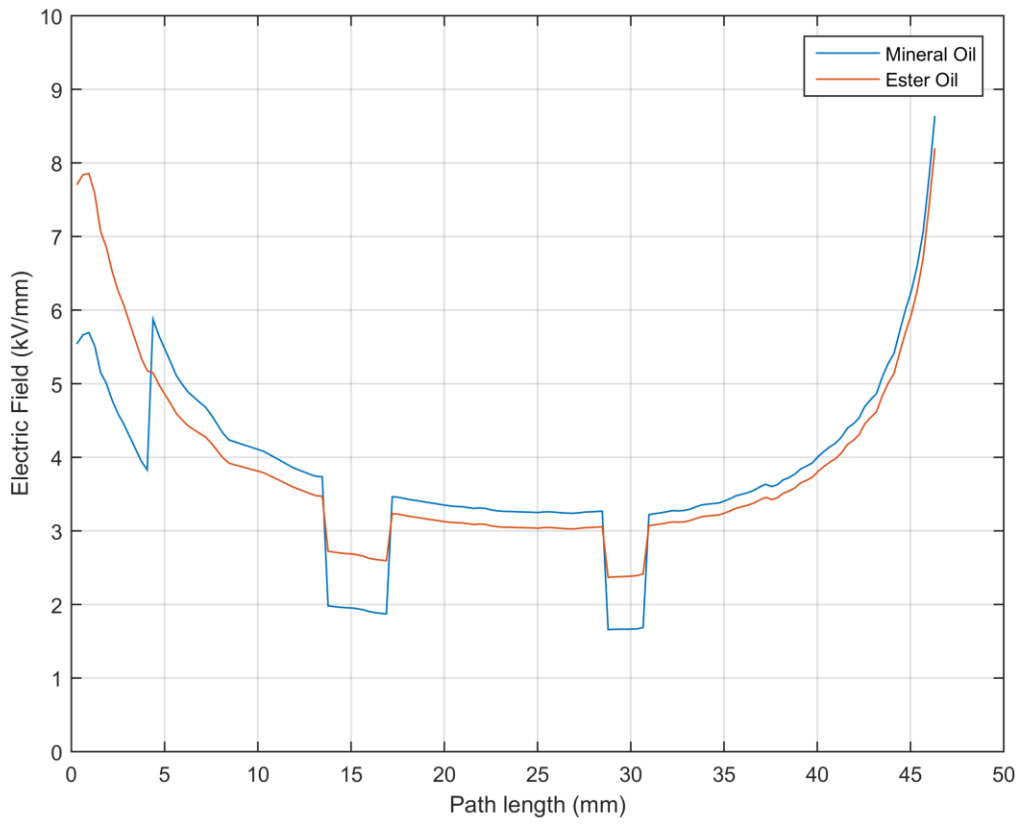


Figure 19-Electric field vs Path Length for mineral and ester oils with improved kraft paper

4.2. Thermal Simulation of Mineral and Ester Based Transformer Winding

Transfer of heat is a key factor of insulating liquids in an operational power transformer. Energy losses in the form of heat are generated from constant re-magnetisation of the core and current flow in the windings. This heat produced is then transferred to surrounding components within the transformer such as the paper, insulating liquid and tank. There are two phenomena's that transfer of heat within a transformer is dependable on [37]. The first phenomenon deals with thermal conductivity of the paper impregnation by oil and the second entails the transfer of heat by oil. Thermal conductivity is defined by the coefficient of the paper whereas the transfer of heat in oil is characterised by the thermal conductivity of the oil, viscosity, density, specific heat capacity and thermal expansion. However natural esters have a higher viscosity than mineral oil that's effects their flow through the ducts and channels designed for cooling in the transformer. The effects of poor cooling within a power transformer result in the insulation materials deteriorating at a rapid rate which will lead to failure. IEEE standards require that the average winding temperature for mineral oil be fixed at 65°C for rated load [38]. It is critical that hot spots on the winding are reduced and eliminated. This section showcases the fluid thermal behaviour of natural ester oil for an 88/6.6 kV 20 MVA transformer. Analysis of the winding velocities and temperature for natural ester oil using COMSOL will be discussed and compared to mineral oil.

The loading (current rating) of a transformer is dependent on the ability of the insulating materials to transfer the heat (created by the losses) away from the windings. Thus the performance of a transformer is effectively determined by the heat transfer equation [39]:

$$\rho C_p \frac{\partial T}{\partial t} - \nabla \cdot (\kappa \nabla T) = q - \rho C_p \vec{v} \cdot \nabla T \quad (16)$$

Where:

T	Temperature [K]
ρ	Density [kg/m ³]
C_p	Specific heat capacity [J/kgK]
t	Time [s]
k	Thermal conductivity [W/mK]
q	Heat generation [W/m ³]
v	Velocity [m/s]

In equation 16, the importance for effective thermal transfer is thermal conductivity (the higher the value the better the heat transfer) and the velocity (the higher the velocity the better the heat transfer). Note that the time dependent term is ignored in this study. The movement is velocity is given by Navier-Stokes equation [39]

$$\rho \left(\frac{\partial \vec{v}}{\partial t} + \vec{v} \cdot \nabla \vec{v} \right) = -\nabla p + \mu \nabla^2 \vec{v} + \frac{1}{3} \mu \nabla (\nabla \cdot \vec{v}) + \rho \vec{g} \quad (17)$$

Where:

- μ Kinematic viscosity [mm²/s]
- p Pressure [Pa]
- g Acceleration [m/s²]

A key component in equation 17 is the viscosity, the lower the viscosity the higher the velocity and thus the higher the heat transfer (equation 16)

Table 17-Thermal Conductivity of Mineral and Ester Oils

Parameter	Thermal Conductivity (W/mK)
Mineral Oil	0.12
Natural Ester	0.17

Table 18-Kinematic Viscosity of Mineral and Ester Oils

Parameter	Viscosity at 40°C (mm ² /s)	Viscosity at 100°C (mm ² /s)
Mineral Oil	9	2.5
Natural Ester	35	8

From Table 17, natural ester oil contains a higher thermal conductivity than mineral oil making it better suited for regulating transformer temperatures. This characteristic allows ester oil to have higher temperature stability than mineral oil. From Table 18, the kinematic viscosity almost four times greater at both 40 °C and 100 °C for natural ester oil. From theory, it implies that transformers with natural ester oil will have hotter winding temperatures than transformers filled with mineral oil.

Darwin et al. considered kinematic viscosity to be the most influential parameter for heat transfer than thermal conductivity. Their experiments reported that transfer of heat by convection within a transformer will be less efficient for natural esters as a higher viscosity produces slower oil flow rates in the winding ducts [5]. Bae et al. team observed that the transformer with an ONAN cooling system, filled with natural ester oil, produced a hot spot temperature of 83 °C making it the worst result from all tests. A slight improvement of 5°C less was reported when an ONAF cooling system was used [7].

Schmidt et al. investigated the thermal performance of a transformer through an experiment and a numerical model using Ansys. They found that for the model the correct boundary conditions are important in predicting the performance of the transformer, where when they set a low temperature and low inlet velocity, their results matched better [40].

Delgado et al. carries out a thermo fluid analysis using a 3D model (COMSOL software) to simulate the temperature and velocities for both natural ester and mineral oil in a winding [41]. His simulations reveal that for temperature, natural ester oil is about 2°C hotter than mineral oil at the top of the winding. However Delgado et al. notices that the outer winding for natural ester oil is cooled better than the inner one with mineral oil. Delgado et al. reports that there will be a higher probability of hot-spot occurrences for vegetable oil due to the oil movements in the vertical and horizontal channels. This is due to the lower Reynolds number found in natural ester oil which determines how well a liquid is able to cool. Analysis of the winding velocity showed that radial channels for both oils were small or negligible. However for the axial winding channels, this changes rapidly for both liquids as the velocity increases to about 60-70 mm/s [41].

Yatsevsky et al. modelled the hydrodynamics and heat transfer in the windings of a power transformer using CFD in Ansys [42]. From his simulation results, Yatsevsky et al. observes self organisation in the hydrodynamic processes with unidirectional oil flow along the numerous horizontal channels between the coils. He considers this a phenomenon and states that it has a considerable influence on the thermal state of the transformer [42]. He also reports that regions of high temperatures are displaced along the winding height and radial direction of velocity.

From the above literature provided by various researchers, some of the important factors to consider when simulating the thermal behaviour of natural ester oil in a winding include proper designing of the winding geometry to compensate for the high viscosity allowing for efficient oil movement as well as velocity measurements within the winding is recommended to determine the heat transfer rate.

4.2.1 Heat Model

The model is based on the high voltage winding of an 88/6.6 kV 20 MVA transformer, where the current density is 3-3.9. The winding is part of a typical HV winding of a distribution power transformer and was modelled in COMSOL. Figure 20 shows the processes required to build the model in COMSOL. The heat transfer in fluids and the laminar flow modules were used (i.e. it has been assumed that the oil does not transition into turbulent flow).

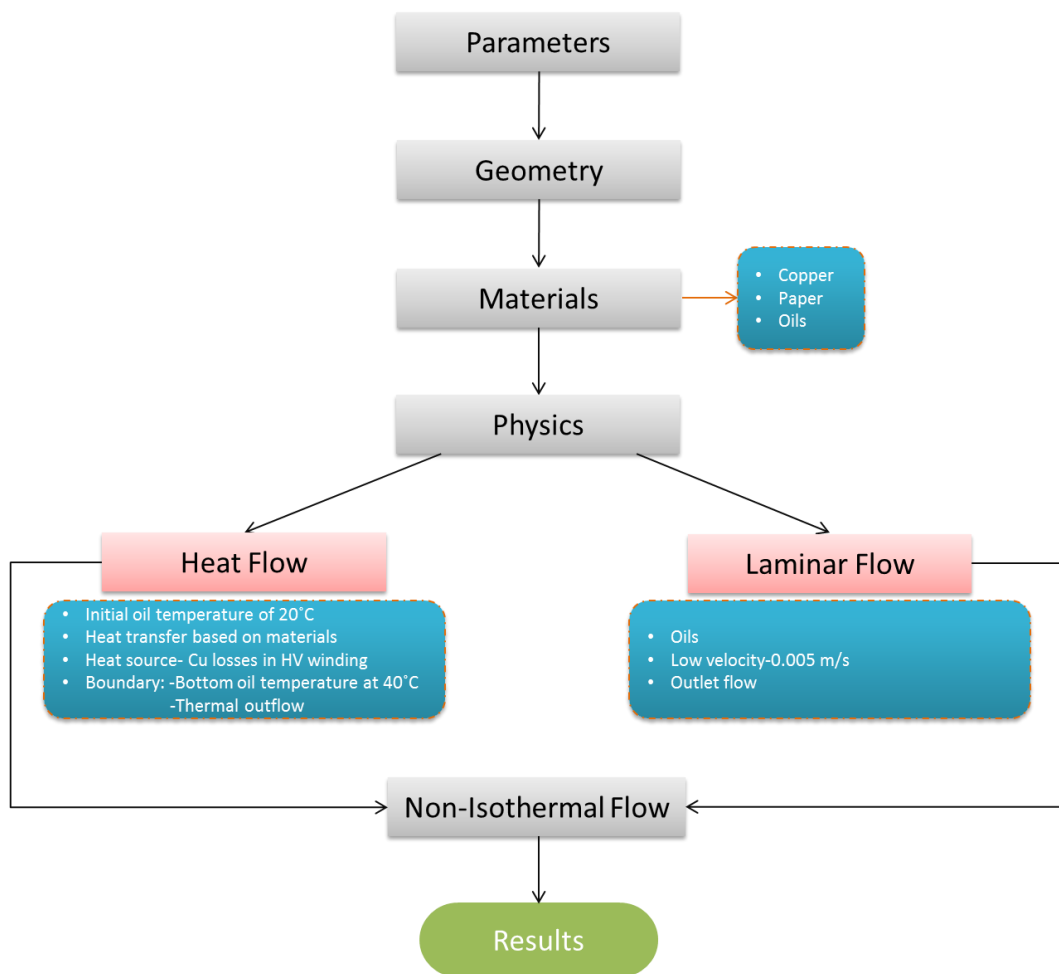


Figure 20-Flowchart showing components required for thermal model

The geometry of the winding based on the following information:

- 35 winding discs were used (approximately a third of a typical winding).
- A 10 mm duct on either side of the winding was assumed.
- A 3 mm space between each disc was assumed.
- A flow washer was used for every 5 discs to force the oil between the windings.

The geometry is illustrated in Figure 21, where the dimensions are in mm and the two red lines indicate the path used to measure the temperature and velocity in the results. The first along the centre of the winding, the second through the duct.

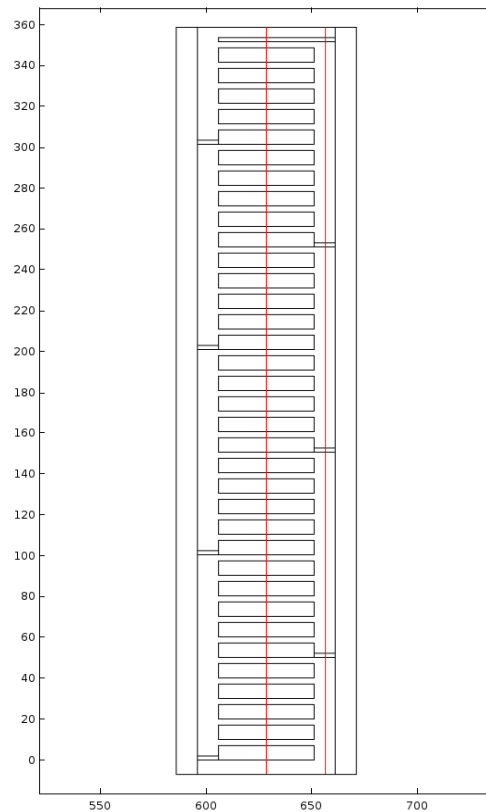


Figure 21- Geometry of Model

The following materials were used:

- The winding discs are modelled as copper (Note that the enamel, resin or paper covering would change the heat transfer characteristics, the purpose of this study was to investigate the oil).
- Pressboard was modelled with a linear thermal conductivity.
- Transformer oil was modelled using the standard transformer oil in the materials library.
- Ester oil was modelled by adjusting the parameters of the standard transformer oil to better fit the information in Tables 17 and 18.

The boundaries were set similarly to Delgado et al. as follows [41]:

- The oil inlet temperature was set to 50°C.
- The heat flux is made by convection at all outlets (i.e. there is no thermal insulation).
- Inlet velocity was varied from 1 to 10 mm/s in the z-direction and 0 mm/s in the r-direction.

- The pressure was fixed at the top.
- The no slip condition was used.

The heat generated on the winding was based on the copper losses of a typical power transformer and a value of 300000 W/cm^3 was used. The model was further set up to be stationary (or time independent).

4.2.2. Heat Model Results

Figure 22 displays the temperature across the winding and the velocity of the oil in the winding. This is for mineral oil with an inlet velocity of 1 mm/s and shows oil entering the bottom of the winding at a temperature of approximately 40°C . As the oil flows up through the windings, heat is absorbed and the temperature rises in the oil. At the top of the winding, the oil reaches a maximum temperature of 74.9°C . This temperature is still within IEEE and IEC limits rated hot spot temperatures which specify 95°C and 97°C respectively, however it must be noted that this is only part of the winding.

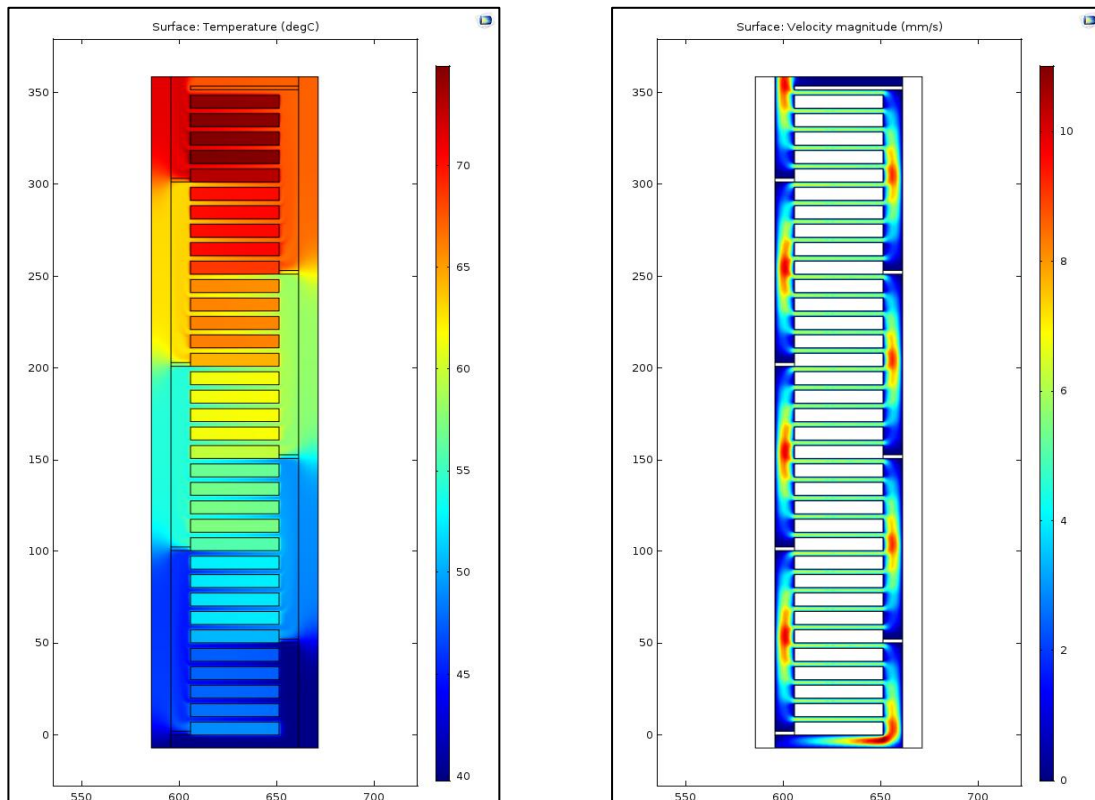


Figure 22-(left) Winding heat distribution for mineral oil; (right) Winding velocity distribution for mineral oil

Figure 24 show that the velocity enters the bottom of the winding at 1 mm/s. It is seen that the velocity increases from 1mm/s to 10mm/s in the vertical ducts which correlates to Delgado et al. research [41].

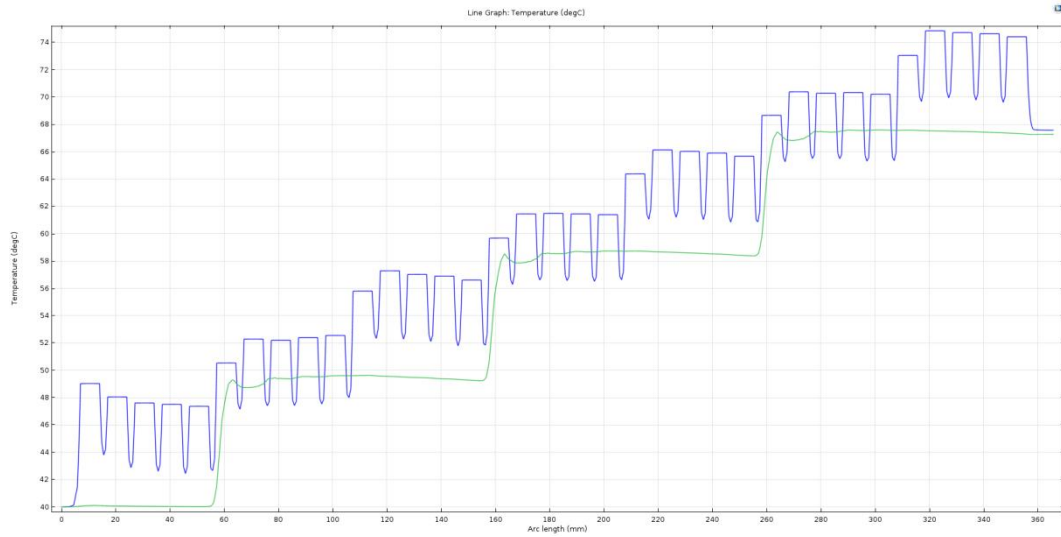


Figure 23-Temperature along central and side paths for inlet velocity of 1 mm/s



Figure 24-Velocity along central and side paths for inlet velocity of 1 mm/s

Tables 19 to 21 summarise the results for mineral and ester oil modules run with inlet velocities of 1 mm/s, 5 mm/s and 10 mm/s.

Table 19-Results for inlet velocity of 1 mm/s

Parameter	Mineral Oil	Ester Oil
Oil temperature (°C)	74.9	74.9
Maximum velocity between discs (mm/s)	9.1	9.2
Maximum Velocity (mm/s)	11	10.9
Minimum Viscosity (mm ² /s)	4.29	15

Table 20-Results for inlet velocity of 5 mm/s

Parameter	Mineral Oil	Ester Oil
Oil temperature (°C)	48.44	48.5
Maximum velocity between discs (mm/s)	47.82	45.7
Maximum Velocity (mm/s)	60.3	55.6
Minimum Viscosity (mm ² /s)	8.4	29.4

Table 21-Results for inlet velocity of 10 mm/s

Parameter	Mineral Oil	Ester Oil
Oil temperature (°C)	44.5	44.7
Maximum velocity between discs (mm/s)	103	94.0
Maximum Velocity (mm/s)	130	116
Minimum Viscosity (mm ² /s)	9.4	32.9

The temperature and velocity plot in Figure 22 indicates that the Multiphysics model is working correctly. The temperature increases from the bottom to top, in line with the direction of flow of the oil. From Tables 19-21, it is observed that natural ester and mineral oil both contain similar oil temperatures and velocities between discs for the same inlet velocity. There is a difference in temperatures and velocities for the different inlet velocities. This illustrates that convective heat transfer due to the velocity of the oil is more important for cooling than the thermal conductivity. While the results for mineral oil and ester are similar in this study for part of a single winding, when considering the entire transformer with radiators, the inlet velocity of the winding may be different due to the differing viscosities.

Delgado et al. showed in their research that the temperature was the highest at the top of the winding and that of the temperature of vegetable oil winding was slightly above that of the mineral oil. They found that the velocity was higher in the vegetable oil than the mineral oil [41]. In comparison to the winding used in this paper, the ester oil had similar temperatures for the different oils, but different velocities for the different oils. If the full winding had been used, a temperature difference may have been evident.

While it is evident that increasing the velocity of the oil is important due to the increased cooling effect, it may lead to other issues. Namely, static electrification is a phenomena related to the flow rate or velocity of the oil [27]. The sizing of the ducting and the spacing of the flow washers are determined so that the flow rate is kept below the required limits. Some early research found flow velocities of an average of 20 cm/s and 45-60 cm/s between discs initiated failures in mineral oil transformers. This is higher than the velocities used in this study.

A few studies have been undertaken for esters, Zelu et al. measured the DC current against flow rate for synthetic and natural esters and compared to that of mineral oil [43]. They found a significantly higher current in the esters indicating the higher charging tendency. Talhi et al. performed experiments that showed that the charging tendency is further influenced by the type of paper, moisture content and ageing by-products [44]. If the velocities are required to be less than that of mineral oil, the heat transferred for the same size of transformer would be less. This needs further investigation to confirm what would happen in a transformer.

4.3. Summary of Design Considerations

In Sections 4.1 and 4.2, only the 88kV winding with respect to the core was modelled. For the dielectric simulations, it is observed that utilising standard kraft paper induces higher stresses (> 9 kV/mm at the top of HV winding) in the paper than the oil. Studies have shown that the insulation on the winding would have to be improved when natural ester oil is used. A simulation emulating thermally upgraded kraft paper (seen in Figure 19) showed a greater improvement on the electric stresses. Therefore, for a natural ester oil based 88/6.6 kV 20 MVA transformer, thermally upgraded kraft paper or paper with a permittivity greater than pressboard must be used. The oil impregnation times for natural ester oils should be increased to accommodate for the higher viscosity and increased paper weight. The use of such paper on the windings will increase the cost of the 88/6.6 kV transformer. The use of stress control rings will alter the winding height as well as the vertical dimensions of the 88/6.6 kV 20 MVA transformer. For streamers (not modelled), electrical designs must be modified such there are larger distances between live and grounded elements. This will further impact the 88 kV transformer as the size will now have to be increased. More metal for the transformer tank and oil will be required. This will once again increase the cost of the transformer.

From the thermal simulations, the 88 kV winding temperatures for natural ester oil were either equal or slightly hotter than mineral oil which correlated to other studies conducted. Also as the inlet velocity increased from the bottom of the winding, the temperature at the top of winding had dropped significantly. For the basic 88 kV transformer mineral oil design, the simulation showed that natural ester oil was still within limits specified by international standards for winding temperatures. This suggests that the 88/6.6 kV 20 MVA mineral oil design transformer does not have to be physically adapted for natural ester oil.

5. Conclusion

Natural esters are a viable alternative to mineral oils, however some important design conclusions included:

- Oil flow is a major factor that influences thermal performance in a winding - Duct sizes, spacers and flow washers would have to be adjusted for natural ester oil due to its high kinematic viscosity property which prompts slower oil flow hence resulting in poor heat transfer from the winding
- It was evident the thermal performance of a typical winding was improved by cooling systems other than ONAN
- The insulation design between LV/HV windings must be analysed in detail and dimensions carefully selected per section as it has a major impact on the dielectric system of a power transformer
- For natural ester oil, most of the dielectric stresses are concentrated at the top of the HV winding. Therefore, mechanisms such as stress control rings and matching of material permittivities is crucial.

These design considerations were investigated by using a generic power transformer design and comparing the thermal and dielectric performance of each.

Chapter 3 covered the design of the 88 / 6.6 kV 20 MVA transformer. All calculations were required to build both dielectric and thermal simulation models. From the design calculations, the following were obtained:

- DIL for LV and HV windings
- Clearances between the core and LV/HV windings
- Number of discs per winding
- LV and HV winding dimensions

In chapter 4 thermal and dielectric models were developed. A Multiphysics model that coupled thermal performance and fluid performance was developed in COMSOL for part of a typical transformer winding. The results of the model displayed the expected results, with the highest temperature occurring at the top of the winding. The boundary conditions were shown to be of high importance as changing the inlet velocity altered the performance of the winding. The difference

between mineral and ester oils is minimal in this particular study. However, it must be noted that the full transformer needs to be considered to have more accurate movement of fluid.

The results from the FEMM simulations conducted showed that the electric field stresses are higher in the paper for ester oil than mineral oil. Natural ester oil could be used in mineral oil designed transformers with a few modifications.

Due to the long gap and streamer propagation in natural ester oil, high electric fields must be minimised as far as possible. Some design suggestions include:

- Using thicker paper for insulation or paper with higher permittivities close to pressboard
- Allowing for larger distances between live and ground parts to cater for the lower breakdown under fast transient voltages in natural ester oils
- Reducing all sharp edges within the transformer
- Apply proper dimensioning principles

The following aspects should be considered for future work:

- A thermal model of the entire transformer using natural ester oil parameters should be considered as this was not modelled in this dissertation. Inclusion of radiators and electrical loading in the system would influence winding temperatures. In these cases, duct sizes for the 88 kV winding as well as the type of cooling system (ONAN, ONAF, ODAF) might vary and require detailed analysis.
- For electrical streamers, also not modelled, clearances and distances between the core/LV/HV windings will have to be investigated as larger distances between live and grounded elements is recommended.

6. References

- [1] T. Marchesan and A. Fanchin, "Natural Ester Fluid: The Transformer Design Perspective," in *IEEE/PES Transmission and Distribution Conference and Exposition (T&D-LA)*, Sao Paulo, 2010.
- [2] IEC 60076-14, "Liquid-immersed power transformers using high-temperature insulation materials," *International Electrotechnical Commission*, 2011.
- [3] R. Fritsche, K. Loppach and F. Trautmann, "EHV Large Power Transformers using Natural Ester Insulation Fluid - Design Challenges and Operation Settings," in *Cigre*, Shanghai, China, 2015.
- [4] Noria Corporation, "Oil Viscosity- How its measured and reported," *Machine Lubrication*, November 2002. [Online]. Available: <http://www.machinerylubrication.com/Read/411/oil-viscosity>.
- [5] A. Darwin, C. Perrier and P. Folliot, "The use of natural ester fluids in transformers," in *Matpost European Conference*, Lyon, 2007.
- [6] T. A. Prevost, "Dielectric Properties of Natural Ester and their influence on Transformer Insulation System Design and Performance," 2009.
- [7] B. Bae, S. Kim, J. Choi, S. Park and Y. Kim, "Design of 154kV power transformer using natural ester oil," in *Cigre*, Paris, 2016.
- [8] EPRI, *Transformer Guide Book Development-The Copper Book*, Palo Alto: EPRI, 2009.
- [9] Actom, *Training Manual- Power Transformers*, Germiston: Actom (Pty) Ltd, 2011.
- [10] Kenji Ookubo, Kenji Ideka, *Recent Power Transformer Technology*, Tokyo: Fuji Electric Company, 1999.
- [11] S. Bisnath, *Eskom Power Book Series- Theory, design , maintenance and life management of power transformers*, Johannesburg: Crown Publications, 2008.
- [12] D. L. Harris, "The Design and Performance of Circular Disc, Helical and Layer Windings for Power Transformer Applications," in *Minnesota Power Systems Conference*, Minnesota, 2009.

- [13] IEC 60076-1, "Liquid-immersed power transformers using high-temperature insulation materials," International Electrotechnical Commission, Geneva, 2013.
- [14] Jim Fitch, "The Enduring Flash Point Test," Noria Corporation, 2000. [Online]. Available: <http://www.machinerylubrication.com/Read/19/flash-point-test>.
- [15] G. Frimpong, S. Page, K. Carrander and D. Cherry, "Transformers transformed," ABB Products, [Online]. Available: <http://www.tdworld.com/sponsored-articles/transformers-transformed>.
- [16] IEC 60296, "Fluids for electrotechnical applications- Unused mineral insulating oils for transformers and switchgear," International Electrotechnical Commission, Geneva, 2003-11.
- [17] D. N. Tanteth, S. Y. Al-Liddawi and D. Ssekasiko, "Properties of Transformer oil that affect efficiency," Blekinge Institute of Technology, Stockholm, 2014.
- [18] IEC 60076-7, "Part 7- Loading guide for oil immersed power transformers," International Electrotechnical Commission, Geneva, 2006.
- [19] IEEE 1538:2000, "IEEE Guide for determination of maximum winding winding temperature rise in liquid-filled transformers," Institute of Electrical and Electronic Engineers, New Jersey, 2000.
- [20] Cargill, "Envirotemp Bulletin B900-00092- Product information," Cooper Power Systems, Pewaukee, 2005.
- [21] Cargill, "Envirotemp FR3 Fluid Testing Guide Section R900-20-12," Cooper Power Systems, Minnesota, 2008.
- [22] M. Materials, "MIDEL eN-Natural Ester Dielectric Insulating Fluid Overview," M&I Materials, Manchester, United Kingdom, March 2014.
- [23] ABB, "BIOTEMP-Biodegradable Dielectric Insulating Fluid," ABB Inc, Boston, 2012.
- [24] Z. Wang, "Experiences in service with new insulating liquids," in *Cigre Conference*, Kyoto, 2011.
- [25] R. Frotscher, Dejan Vukovic, "Behaviour of Ester Liquids under Dielectric and Thermal Stress- From Laboratory Testing to Practical Use," in *Cigre*, Paris, 2012.
- [26] G. Dombek, P. Goscinski and Z. Nadolny, "Comparison of mineral oil and esters as cooling liquids in high voltage transformer in aspect of environment protection," *Energy and Fuels*, vol. 14,

2016.

- [27] S. Kulkarni and S. Khaparde, *Transformer Engineering - Design and Practice*, Marcel Dekker, 2004.
- [28] J. K. Nelson, "An assessment of the physical basis for the application of design criteria for dielectric structures," *IEEE Transactions on Electrical Insulation*, vol. 24, no. 5, 1989.
- [29] W. Ziomek, K. Vijayan, D. Boyd, K. Kuby and M. Franchek, "High voltage power transformer insulation design," *2011 Electrical Insulation Conference (EIC)*, Annapolis, MD, 2011.
- [30] J. Nelson and C. Shaw, "The Impulse Design of Transformer Oil-Cellulose Structures," *IEEE Transactions on Dielectric and Electrical Insulation*, 2006.
- [31] Cooper Power Systems, "Envirotemp FR3 Fluid," Cooper Industries, Wisconsin, 2001.
- [32] K.Rapp, C.Mcshane, J.Vandermaar, D. Vukovic and S.Tenbohlen, "Long Gap Breakdown of Natural Ester Fluid," in *International Conference on High Voltage Engineering and Application*, New Orleans, 2010.
- [33] C. Duy, O.Lesaint, A.Denat and N. Bonifaci, "Streamer Propagation and Breakdown in Natural Ester at High Voltage," *IEEE Transactions on Dielectric and Electrical Insulation*, 2009.
- [34] Z.D Wang, Q.Lui, "Streamer Characteristic and Breakdown in Synthetic and Natural Ester Transformer Liquids with Pressboard Interface under Lightning Impulse Voltage," *IEEE Transactions on Dielectrics and Electrical Insulation*, 2011.
- [35] Chakraborty, Biswas and Sudha, "Analysis of Power Transformer Insulation using FEM," *International Journal of Soft Computing and Engineering (IJSCE)*, vol. 2, no. 3, 2012.
- [36] Danilo Makuc, Juso Ikanovi, Konrad Lensai, "Electric field analysis of insulation structure of power transformers," *Computer Engineering in Applied Electromagnetism*, 2003.
- [37] P. Gościński, "Analysis of heat transfer coefficient of synthetic and natural ester in the aspect of their application in power transformers," *Rocznik*, vol. 13, 2015.
- [38] IEEE C57.91, "Guide for loading Mineral-Oil-Immersed Transformers and Step-Voltage Regulators," IEEE, New Jersey, 2011.

- [39] COMSOL, "Heat Transfer Module User's Guide," *COMSOL Multiphysics*, 2017.
- [40] N. Schmidt, S. Tenbohlen, S. Chen and C. Breuer, "Numerical and experimental investigation of the temperature distribution inside oil-cooled transformer winding," *International Symposium on High Voltage Engineering, Seoul, Korea, 2013*.
- [41] Unsal, Delgado, Fernandez, Urquiza and Mumyakmaz, "Fluid-thermal analysis of the cooling capacity of a commercial natural ester in a power transformer," in *International Conference on Renewable Energies and Power Quality, 2013*.
- [42] V.Yatevsky, "Hydrodynamics and heat transfer in cooling channels of oil filled power transformers with mutlicoil windings," *Applied Thermal Engineering*, vol. 63, 2014.
- [43] Y. Zelu, T. Paillat, G. Morin, C. Perrier and M. Saravolac, "Study on flow electrification hazards with ester oils," *2011 IEEE International Conference on Dielectric Liquids, Trondheim, 2011*.
- [44] M. Talhi, I. Fofana and S. Flazi, "Comparative study of the electrostatic charging tendency between synthetic ester and mineral oil," *IEEE Transactions on Dielectrics and Electrical Insulation*, vol. 20, no. 5, 2013.

Appendix A

A.1. FEMM Dielectric Simulations

Simulation 1

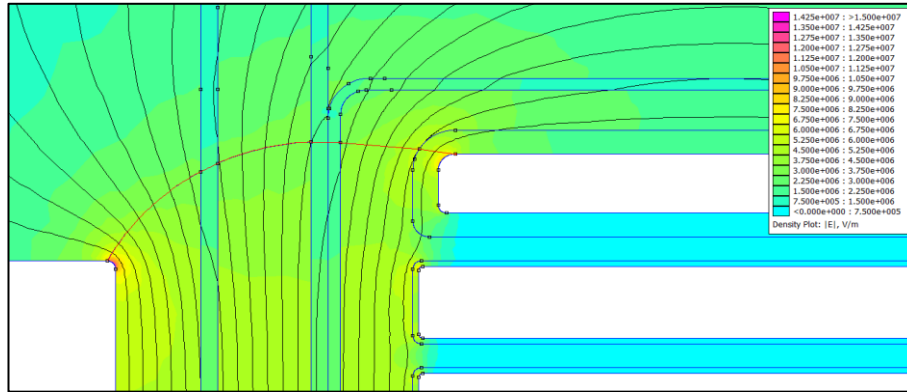


Figure 25- Mineral Oil (HV to LV winding path_Top section)

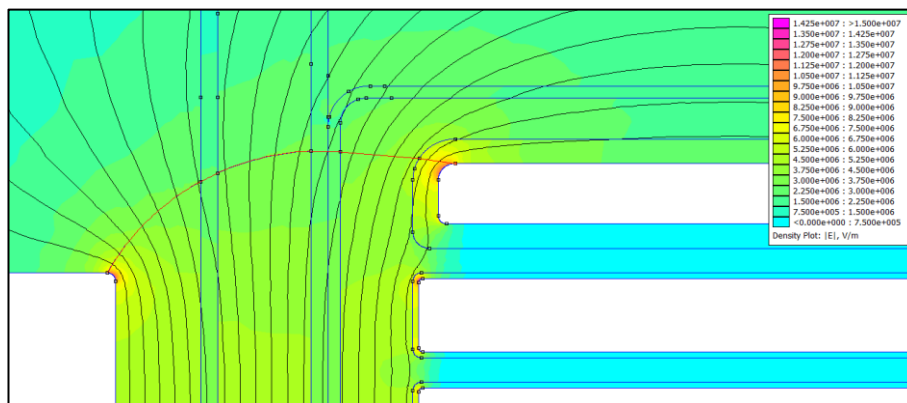


Figure 26-Ester Oil (HV to LV winding path_Top section)

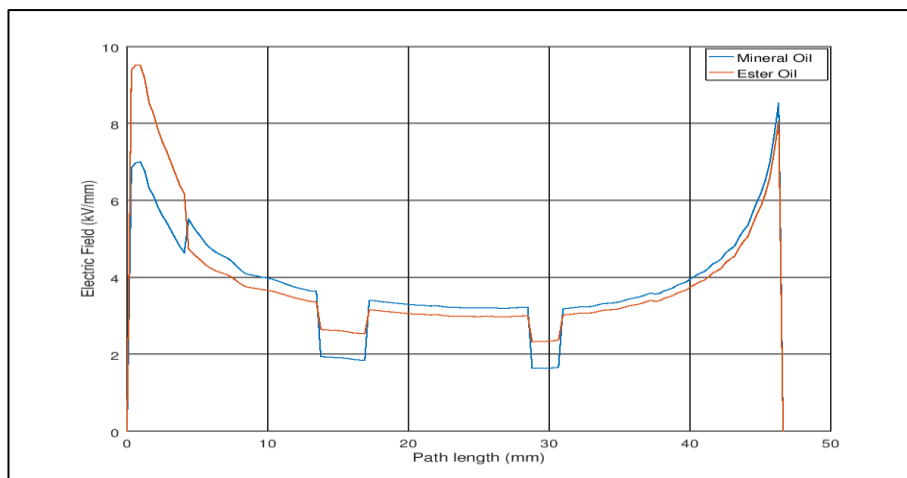


Figure 27-Electric field vs Path Length (HV to LV winding path_Top section)

Simulation 2

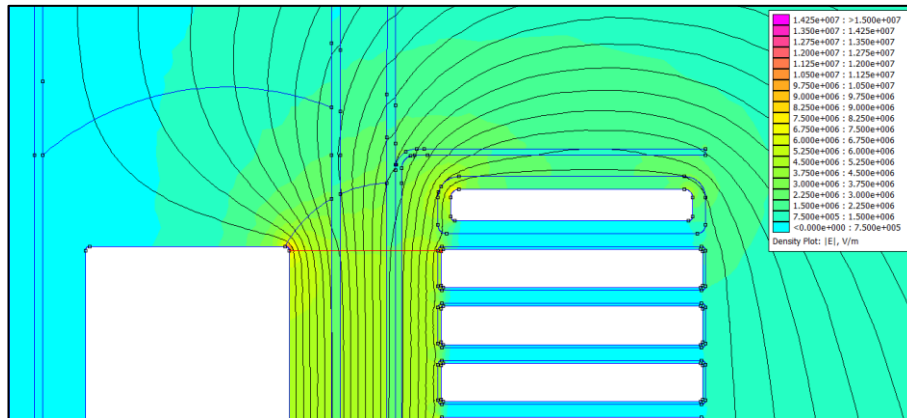


Figure 28-Mineral Oil (HV to LV winding path_Top section)

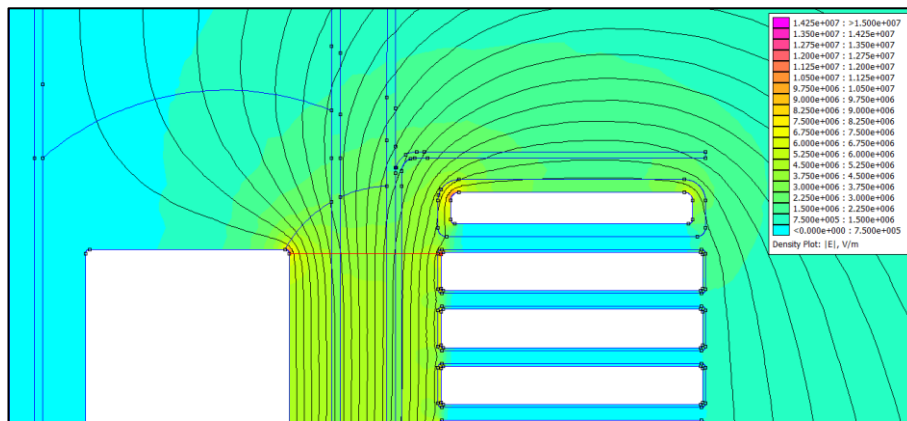


Figure 29-Ester Oil (HV to LV winding path_Top section)

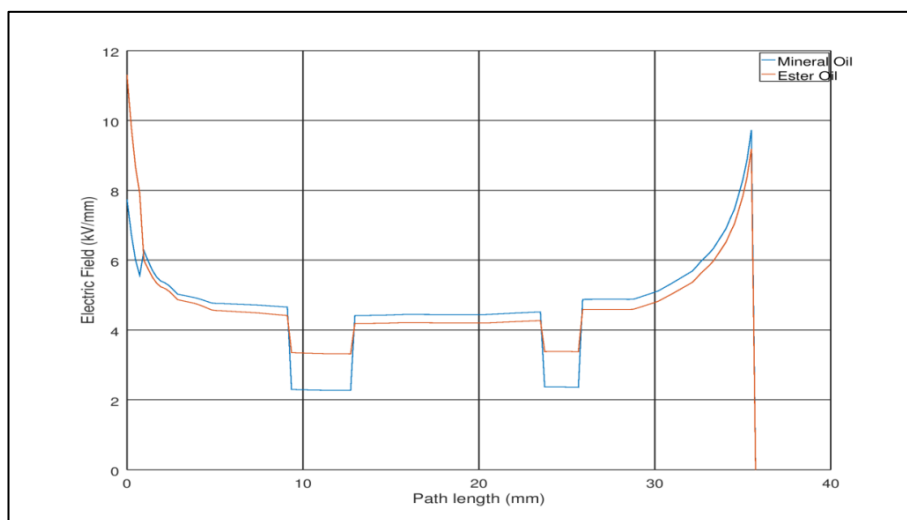


Figure 30-Electric field vs Path Length (HV to LV winding path_Top section)

Simulation 3

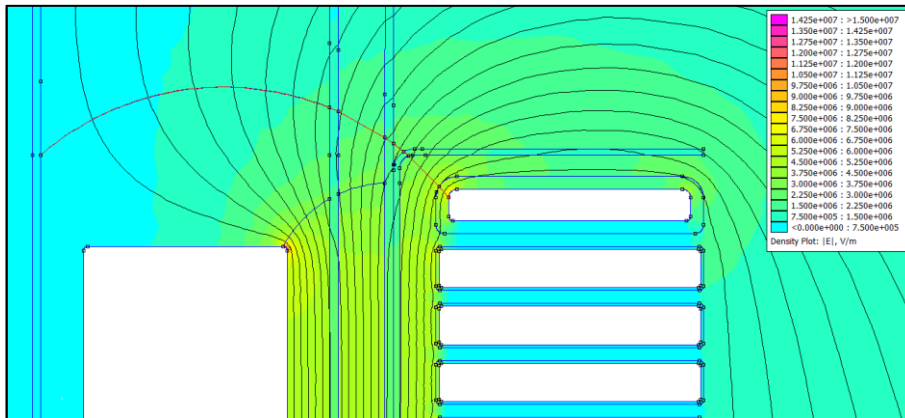


Figure 31-Mineral Oil (HV winding to Core path)

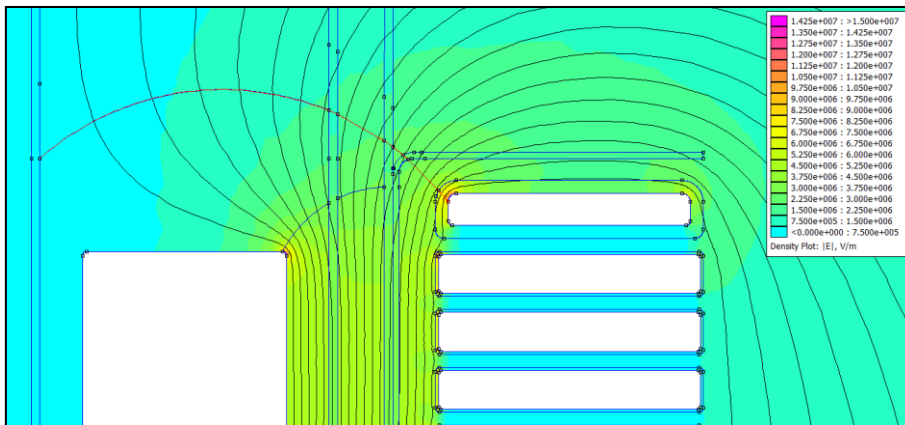


Figure 32-Ester Oil (HV winding to Core path)

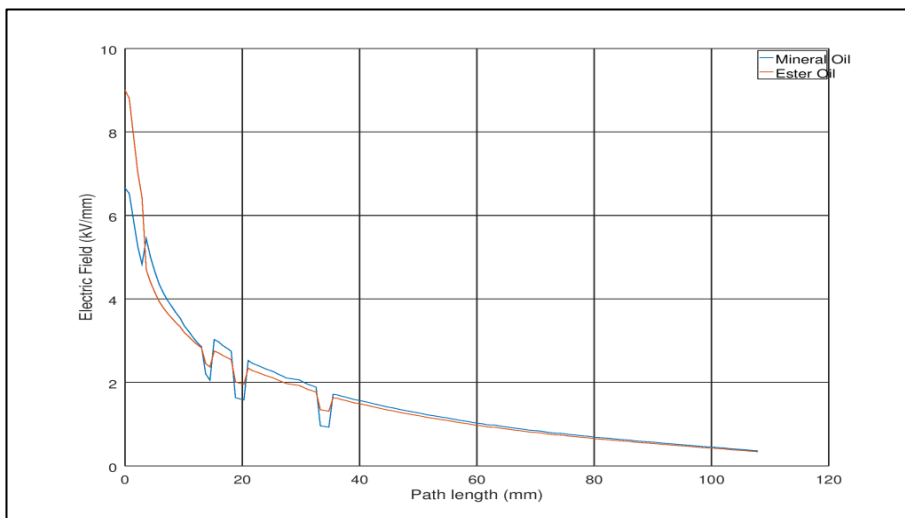


Figure 33-Electric field vs Path Length (HV winding to Core path)

Simulation 4

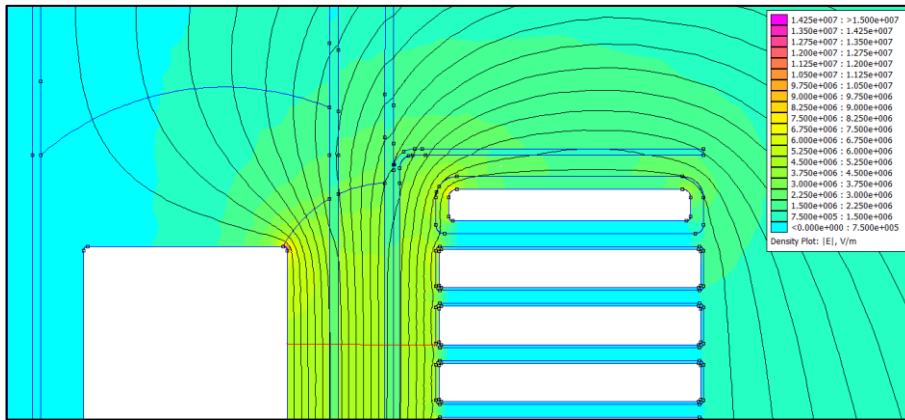


Figure 34-Mineral Oil (HV to LV winding path_Top section_2nd winding disc)

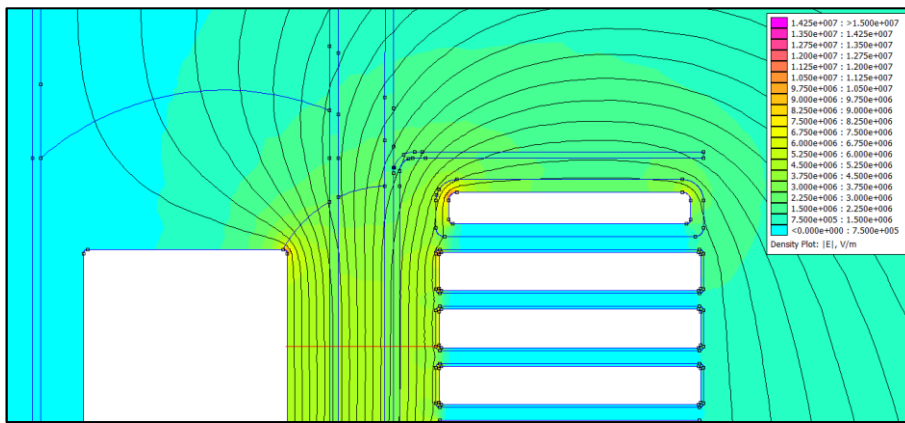


Figure 35-Ester Oil (HV to LV winding path_Top section_2nd winding disc)

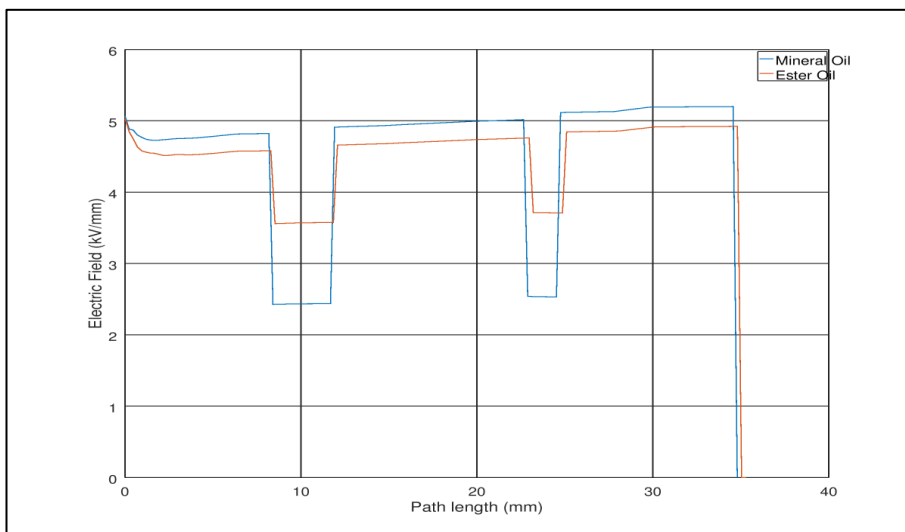


Figure 36-Electric field vs Path Length (HV to LV winding path_Top section_2nd winding disc)

Simulation 5

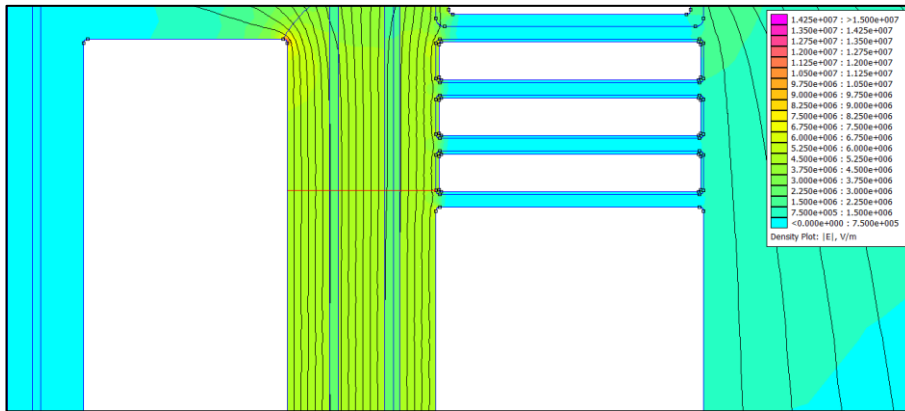


Figure 37-Mineral Oil (HV to LV winding path_Top section_3rd winding disc)

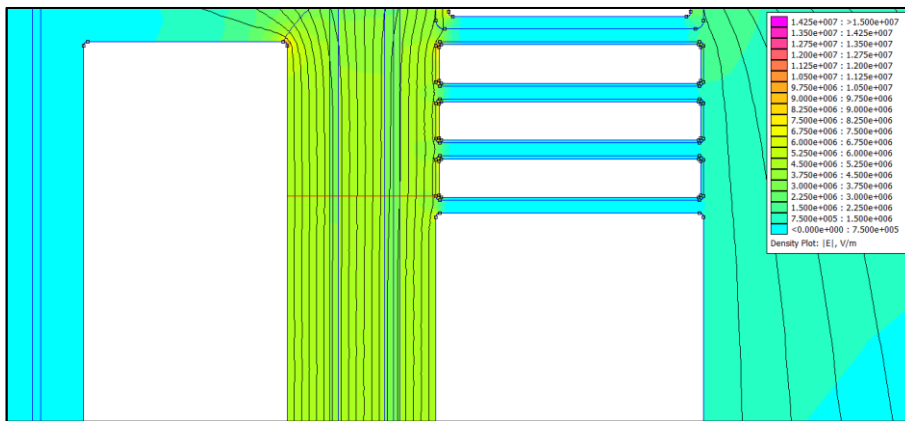


Figure 38-Ester Oil (HV to LV winding path_Top section_3rd winding disc)

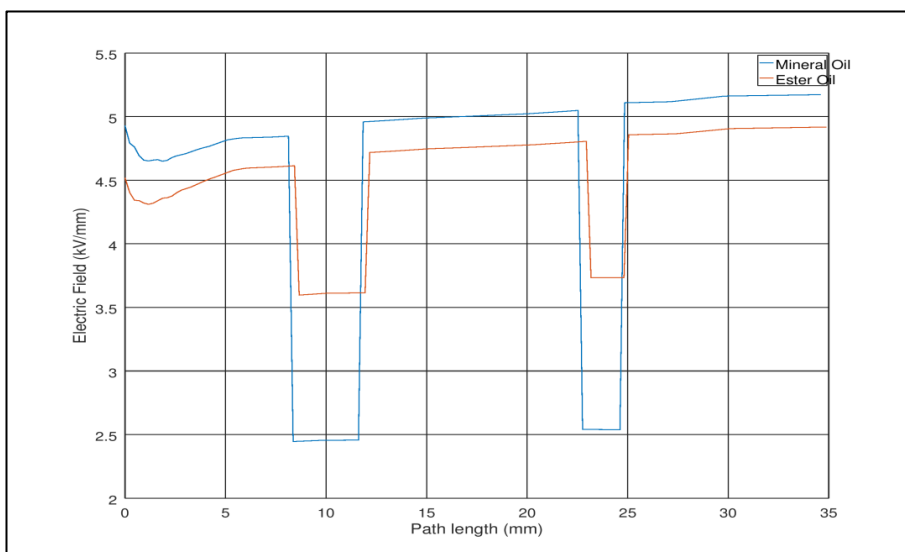


Figure 39-Electric field vs Path Length (HV to LV winding path_Top section_3rd winding disc)

Simulation 6

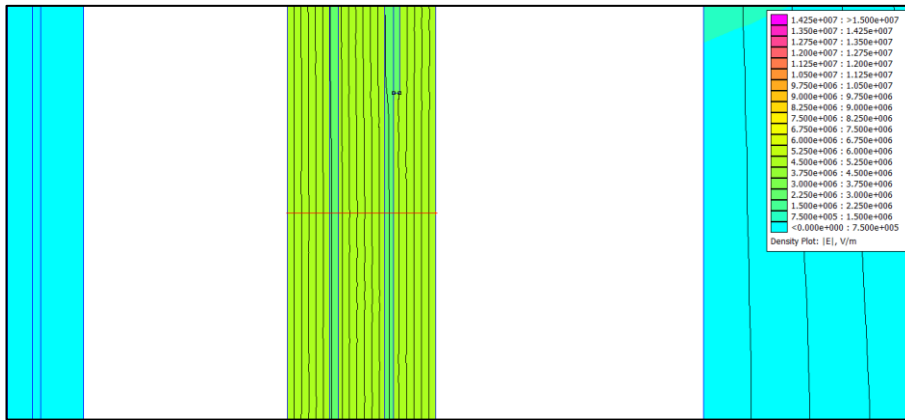


Figure 40-Mineral Oil (HV to LV winding path_Middle section)

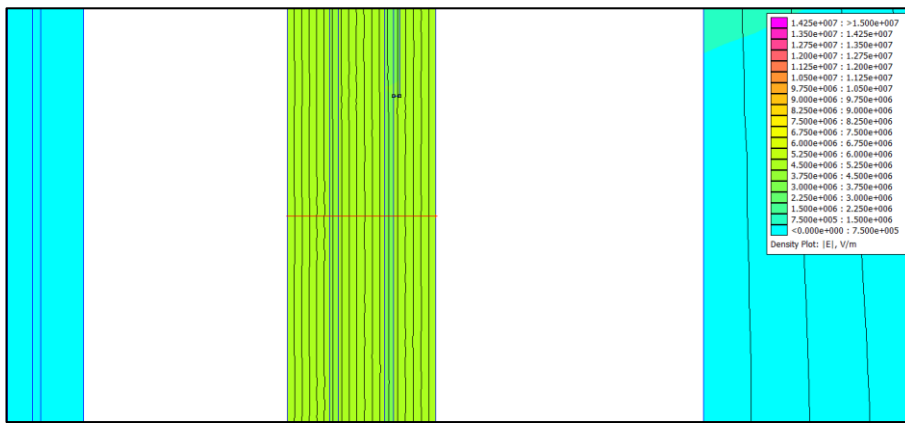


Figure 41-Ester Oil (HV to LV winding path_Middle section)

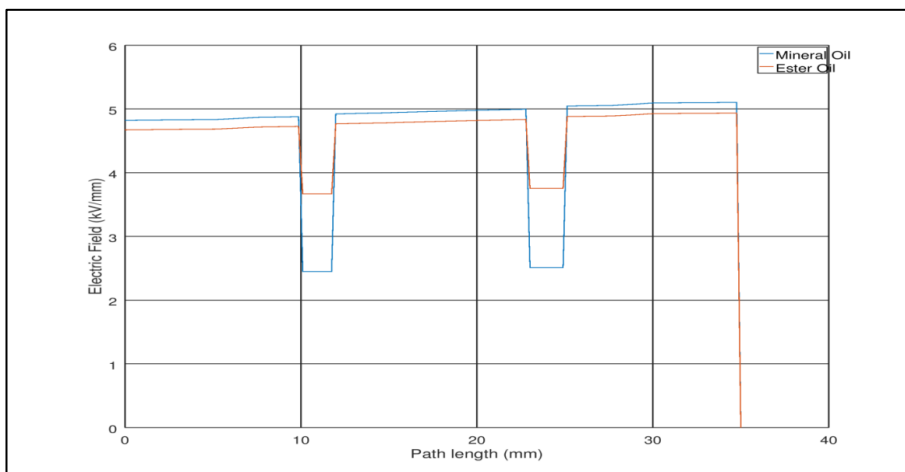


Figure 42-Electric field vs Path Length (HV to LV winding path_Middle section)

Simulation 7

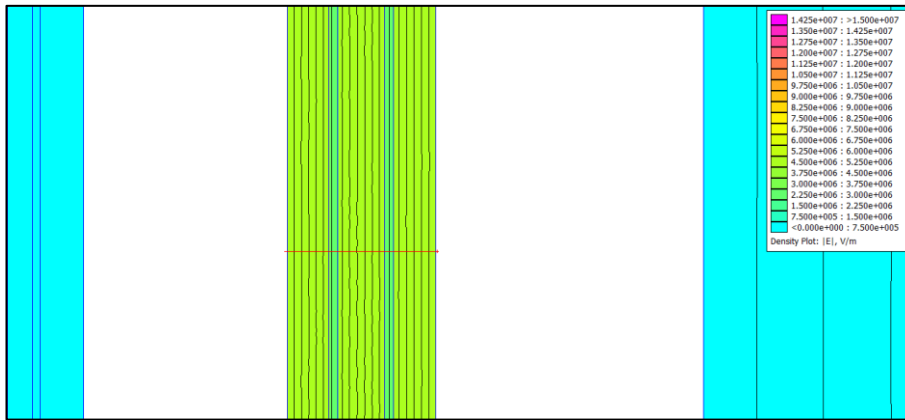


Figure 43-Mineral Oil (HV to LV winding path_Middle section)

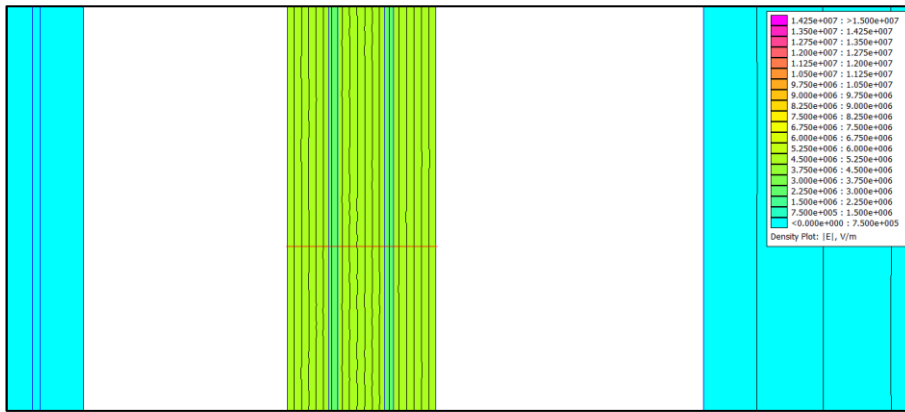


Figure 44-Ester Oil (HV to LV winding path_Middle section)

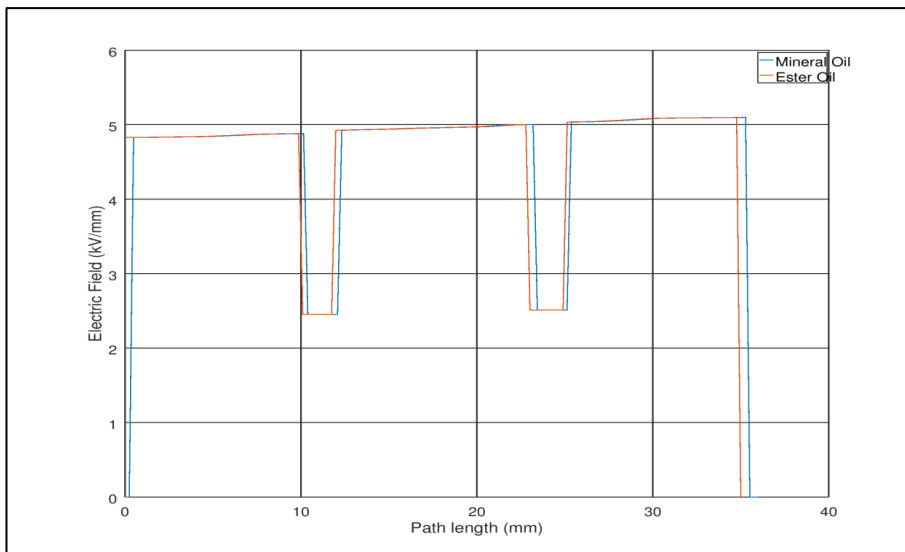


Figure 45-Electric field vs Path Length (HV to LV winding path_Middle section)

Simulation 8

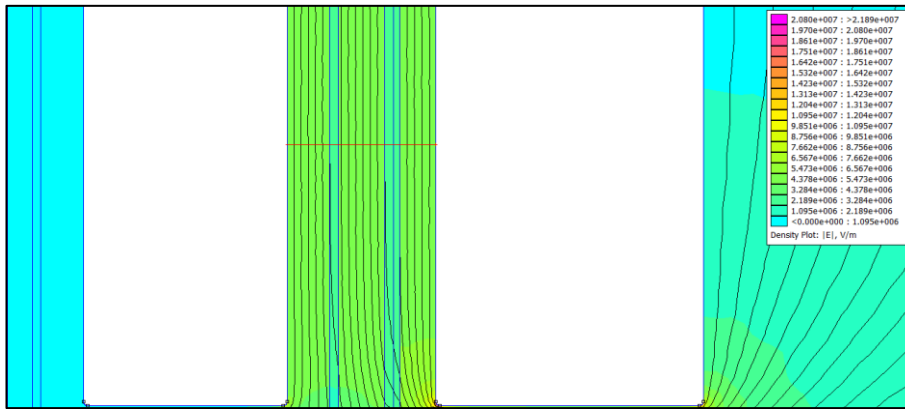


Figure 46-Mineral Oil (HV to LV winding path_Bottom section)

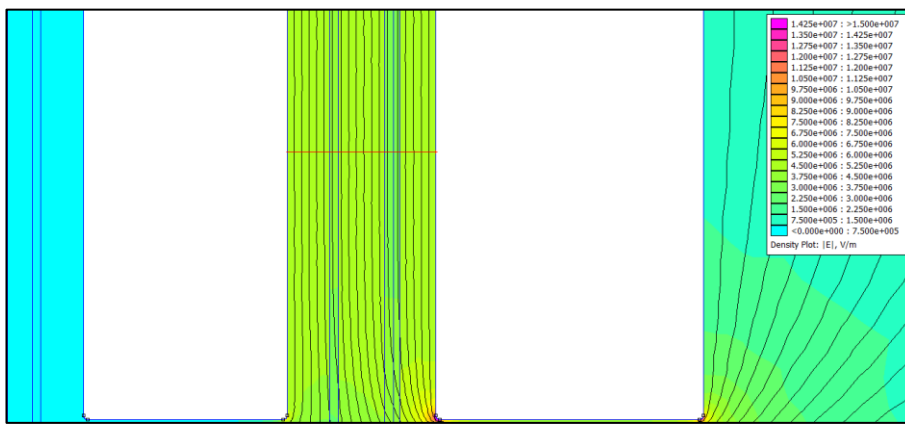


Figure 47-Ester Oil (HV to LV winding path_Bottom section)

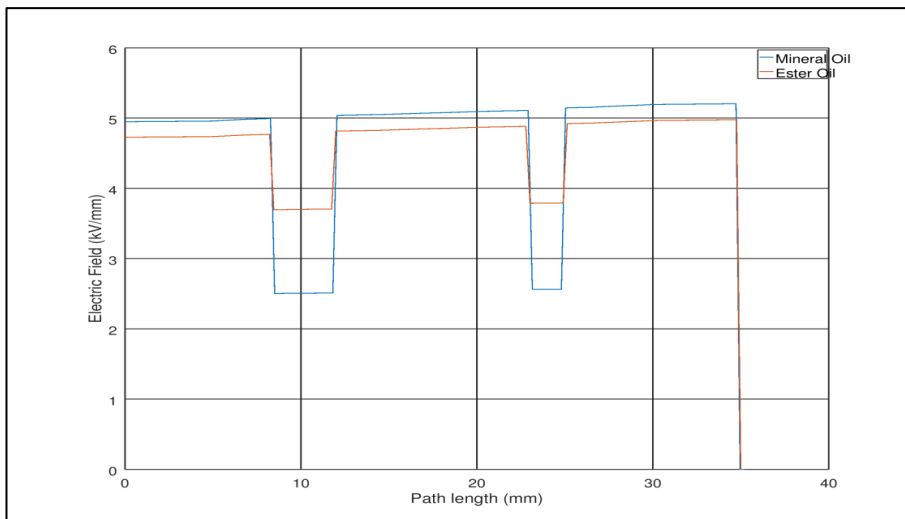


Figure 48-Electric field vs Path Length (HV to LV winding path_Bottom section)

Simulation 9

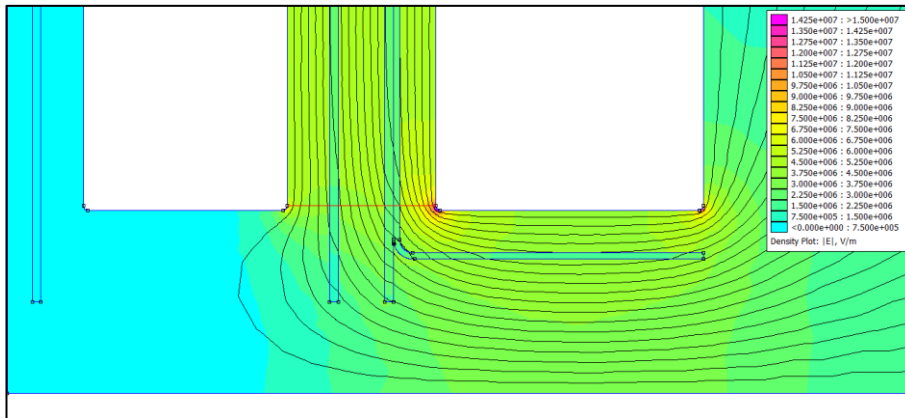


Figure 49-Mineral Oil (HV to LV winding path_Bottom section)

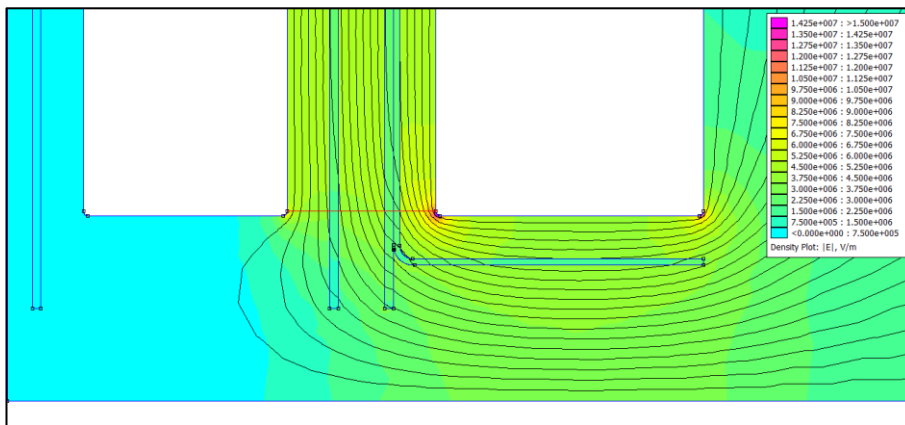


Figure 50-Ester Oil (HV to LV winding path_Bottom section)

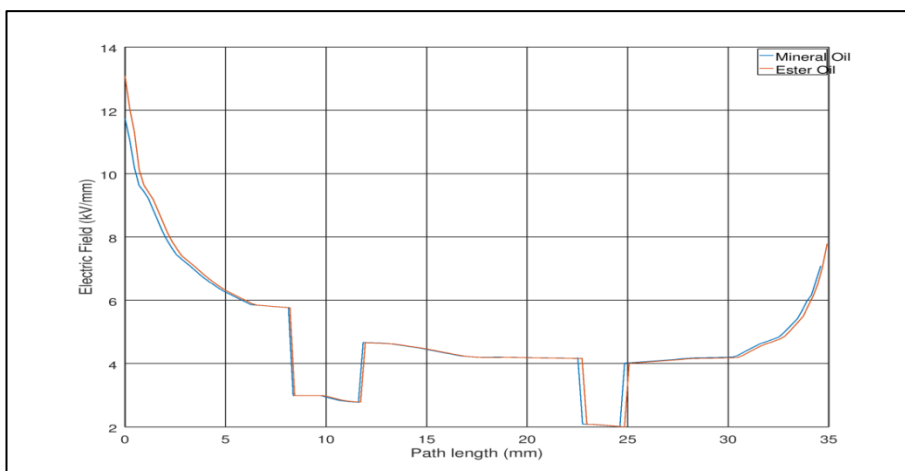


Figure 51-Electric field vs Path Length (HV to LV winding path_Bottom section)

Simulation 10

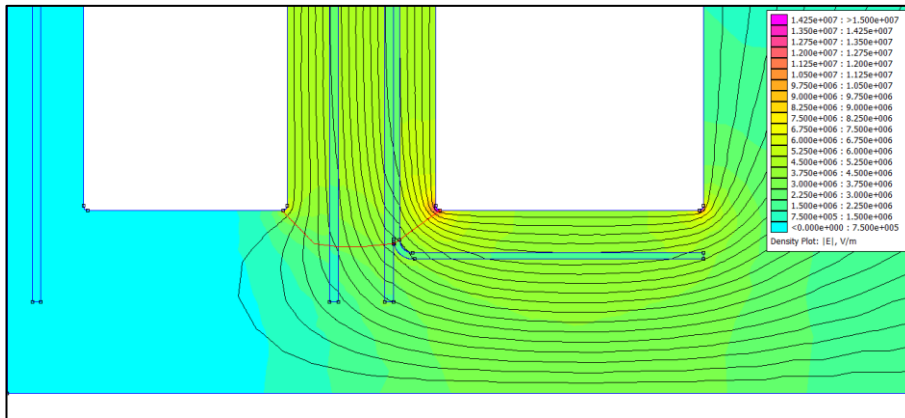


Figure 52-Mineral Oil (HV to LV winding path_Bottom section)

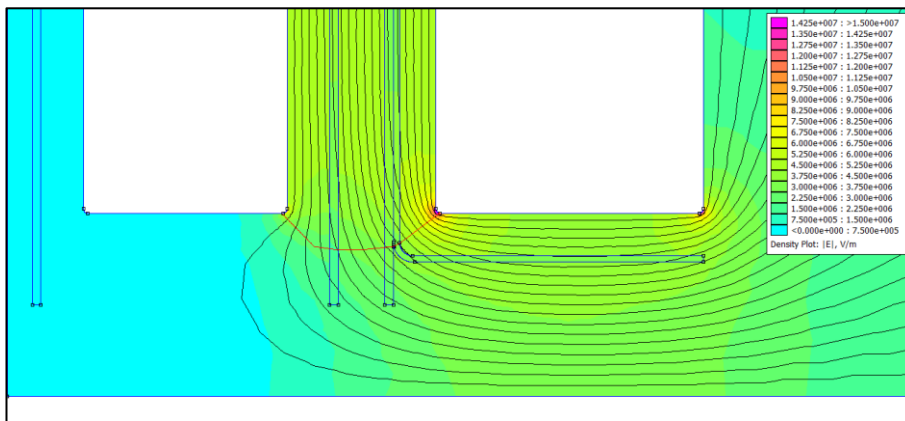


Figure 53-Ester Oil (HV to LV winding path_Bottom section)

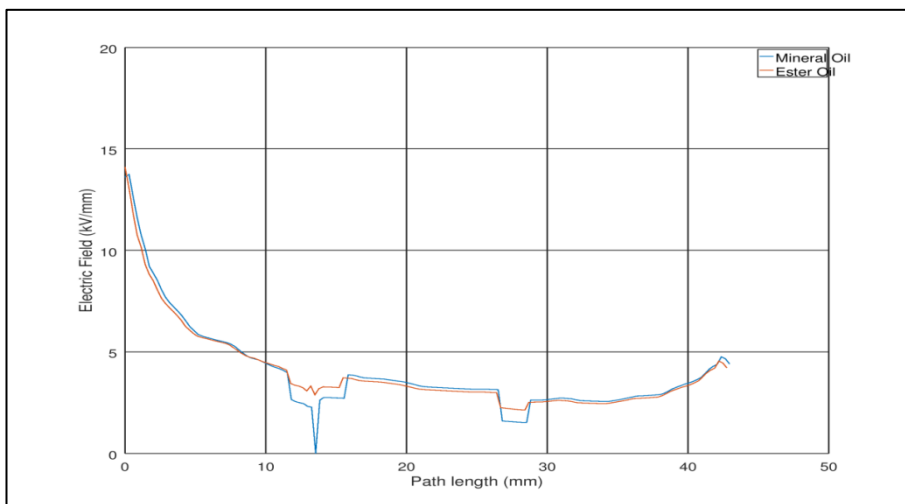


Figure 54-Electric field vs Path Length (HV to LV winding path_Bottom section)

Simulation 11

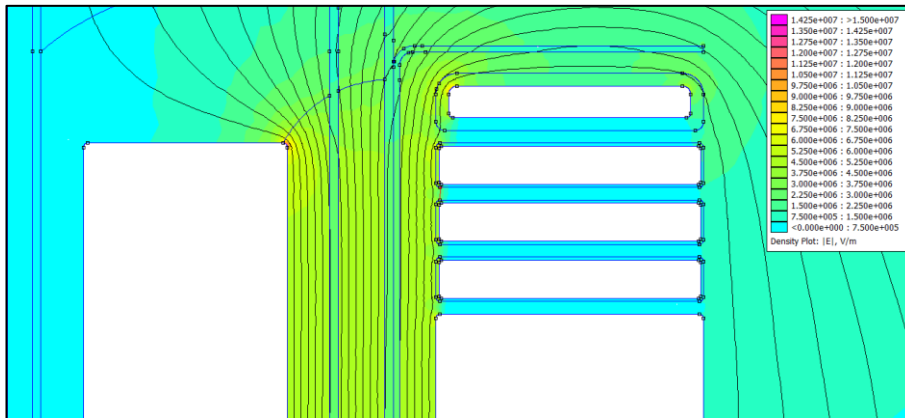


Figure 55-Mineral Oil (HV to HV winding_1st winding disc to 2nd winding disc)

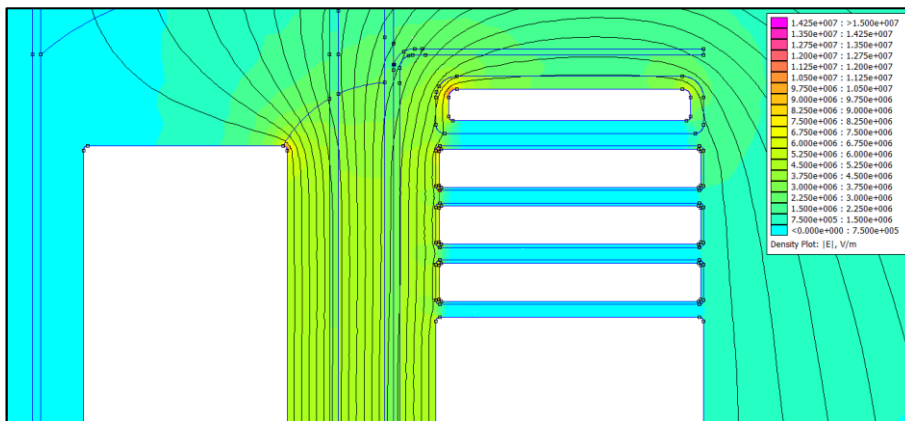


Figure 56-Ester Oil (HV to HV winding_1st winding disc to 2nd winding disc)

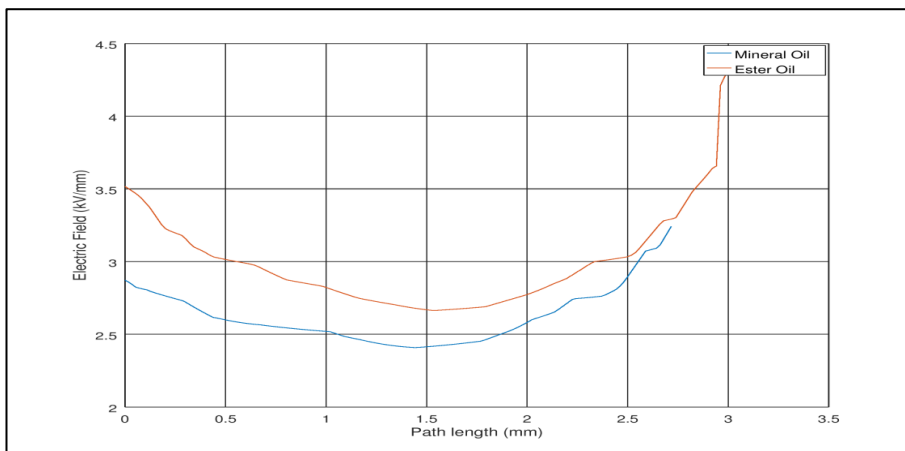


Figure 57-Electric field vs Path Length HV to HV winding_1st winding disc to 2nd winding disc)

A.2. Dielectric simulation code using Octave 4.2.1 software

```
clear

file1 = dlmread('mineral_LVC.txt',' ',2,0);
file2 = dlmread('ester_LVC.txt',' ',2,0);

% Gap withstand

d1 = real(file1(:,1));
E1 = imag(file1(:,1))/1000/1000;
d2 = real(file2(:,1));
E2 = imag(file2(:,1))/1000/1000;
Ew1 = zeros(size(d1));

a1 = 72;
Ew1(1:a1,1) = 18*d1(1:a1,1).^0.38;

a1 = 40;
a2 = 90;
Ew1(a1:a2,1) = 18*(d1(a1:a2,1)-d1(a1,1)).^0.38;

a1 = 50;
a2 = 90;
Ew1(a1:a2,1) = 18*(d1(a1:a2,1)-d1(a1,1)).^0.38;

figure(1),plot(d1,E1,d2,E2)

xlabel('Path length (mm)'),ylabel('Electric Field (kV/mm)'),
legend('Mineral Oil','Ester Oil'), grid on

print('path 18.png','-dpng','-r300')

% Creep withstand

d1 = file1(:,1);
E1 = file1(:,2)/1000/1000;
Ec1 = zeros(size(d1));

a1 = 72;
Ec1(1:a1,1) = 15*d1(1:a1,1).^0.37;

figure(2),plot(d1,E1,d1,Ec1)

xlabel('Path length (mm)'),ylabel('Electric Field (kV/mm)'),
```



```
legend('Mineral Oil','Ester Oil','Withstand')
```

A.3. 88/6.6kV 20MVA Transformer calculation code using Octave 4.2.1 software

```
clear;
```

```
% Ratings
```

```
% Design for Mineral Oil
```

```
% 20 MVA 88kV/6.6kV YNd1 OLTC +5% -15% , Z%= 10% , 50Hz , 1.718T
```

```
% 88kV BIL specs: LI 380kV , ASCD 150kV , AC 95kV
```

```
% 6.6kV BIL specs: LI 75kV , ACSD 13.2kV , AC 22kV
```

```
disp(' ')
```

```
disp('Ratings')
```

```
disp(' ')
```

```
S = 20e6;      % MVA
```

```
V1 = 88e3;    % V_HV
```

```
V2 = 6.6e3;   % V_LV
```

```
f = 50;       % Hz
```

```
% Current Calculations
```

```
I1 = S/(V1*sqrt(3));      % HV_A_Tap 5
```

```
I2 = (S/(V2*sqrt(3)))/sqrt(3); % LV_A
```

```
I3 = S/(sqrt(3)*(0.85*V1)); % HV_A_Tap 17
```

```
% Design Flux
```

```
B = 1.718      % T
```

```
%%%%%%%%%%%%%%%%%%%%%%%%%%%%%%%%%%%%%%%%%%%%%%%%%%%%%%%%%%%%%%%%%%%%%%%%
```

```
% Core details
```

```
% Core material 30R122
```

```
disp(' ')
```

```
disp('Core')
```

```
disp(' ')
```

```
core_d = 40*(S/1000)^(0.25); % core diameter mm
```

```
core_a = pi*core_d^2/4; % core cross-sectional area
```

```
ff = 0.72; % fill factor
```

```
core_a = ff*core_a/1000^2;
```

```
v_per_turn = 4.44*B*f*core_a % volts per turn
```

```
%%%%%%%%%%%%%%%%%%%%%%%%%%%%%%%%%%%%%%%%%%%%%%%%%%%%%%%%%%%%%%%%%%%%%%%%
```

```
% Min oil clearances - Design Insulation Level
```

```
disp(' ')
```

```
disp('Clearances')
```

```
disp(' ')
```

```
BIL1 = 380; % kV
```

```
BIL2 = 75; % kV
```

```
DIL = 5.7; % kV/mm
```

```
DILf = 2.65; % Converts to BIL equivalent RMS level
```

```
ES1 = BIL2/DILf %Electric stresses for LV kV
```

```
ES2 = BIL1/DILf %Electric stresses for HV kV
```

```
% From calculations we choose 28kV for LV = ES1 value
```

```
% From calculations we choose 150kV for HV = ASCD value
```

```

%%%%%%%%%%
% Check HV & LV BIL specs

% Based on values of ES1 and ES2

C_LV = 16;    %clearance between Core and LV winding mm
LV_HV = 31;   %clearance between LV and HV winding mm
HV_Tap = 32;  %clearance between HV and Tap winding mm

ES_LV = ES1/C_LV; % Eskom check LV: value must be below 5.7 kv/mm
ES_HV = 150/LV_HV; % Eskom Check HV: value must be below 5.7 kv/mm
ES_Tap = 150/HV_Tap; % Eskom Check Tap: value must be below 5.7 kv/mm

%%%%%%%%%%

% HV Conductor details

disp(' ')
disp('HV Conductors')
disp(' ')

J1 = 3.7;           % Design current density HV A/mm2
Ac1 = I3/J1;       % Cross section area mm2
Ac1_w=2.2;        % 9.7 x 2.2 mm - Need to choose here
Ac1_h=9.7;
P1 = 0.7;         % Paper covering mm - 1.25+/-5%
Ac1_w = Ac1_w+P1;
Ac1_h = Ac1_h+P1;

WH_HV = 1555;     % Window height given by manufacturer mm
Spacer1 = 3;      % mm

Num_Turns_HV = ((V1*0.85)/sqrt(3) )/v_per_turn; % Number of turns on HV
MH_HV = (Num_Turns_HV/9*Spacer1)+(Num_Turns_HV/9*Ac1_h); % MH calculation for HV
Num_discs_HV = MH_HV/Ac1_h; %Number of discs on HV winding
Rad_b_HV = 53; %Radial build HV winding given by manufacturer mm

```

%%%

% LV Conductor details

disp('')

disp('LV Conductors')

disp('')

J2= 3.1; % Design current density LV A/mm2

Ac2 = I2/J2

Ac2_w=3.4; % 7.1 x 3.4 mm - Need to choose here

Ac2_h=7.1;

P2 = 0.6; % Paper covering mm - 0.7+/-5%

Ac2_w = Ac2_w+P2;

Ac2_h = Ac2_h+P2;

WH_LV = 1555; % Window height given by manufacturer

Spacer2 = 2; % mm

Num_Turns_LV = V2/v_per_turn; % Number of turns on HV

MH_LV = (Num_Turns_LV*Spacer2)+(Num_Turns_LV*Ac2_h); %MH calculation for LV

Num_discs_LV = MH_LV/Ac2_h;

Rad_b_LV = 57; %Radial build LV winding mm

%%

% Tap Conductor details

disp(' ')

disp('Tap Conductors')

disp(' ')

J3= 4; % Design current density LV A/mm2

Ac3 = I3/J3

Ac3_w=4.4; % 8.9 x 4.4 mm

Ac3_h=8.9;

P3 = 2; % Paper covering mm

Ac3_w = Ac3_w+P3;

Ac3_h = Ac3_h+P3;

Num_Turns_Tap = (((V1*1.05)-(V1*0.85))/sqrt(3))/v_per_turn; % Number of turns on HV

WH_Tap = 1555; % Window height given by manufacturer

MH_Tap = 1271;

Num_discs_Tap = MH_Tap/Ac3_h;

Rad_b_Tap = 13; %Radial build Tap winding mm

%%

% HV - LV

disp(' ')

disp('Ducts')

disp(' ')

CW2 = ES1/DIL % clearance between core and LV mm

CW1 = ES2/DIL % clearance between core and HV mm

CW1W2 = BIL1/DILf/DIL % clearance between LV and HV mm

CWAWB = BIL1*sqrt(3)/DILf/DIL; % clearance between phases mm

Ducts1 = CW1W2/12; % Max distance of oil gaps is 12 mm

Board1 = 2; % 2 mm

Ducts1 = (CW1W2-round(Ducts1)*Board1)/12; % Include the pressboard 1.5-2mm

E1av = BIL1/DILf/(CW1W2-0.5*3*Board1);